MICROCOPY RESOLUTION TEST CHART

NATIONAL BUREAU OF STANDARDS-1963-A

AD-A145 752

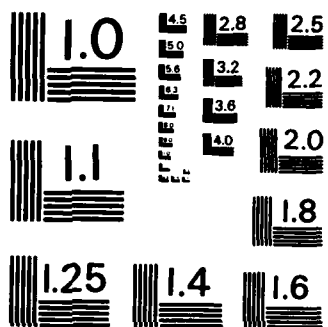DTNSRDC–84/025

DAVID W. TAYLOR NAVAL SHIP
RESEARCH AND DEVELOPMENT CENTER

Bethesda, Maryland 20084

COMPARISON OF PREDICTED AND MEASURED FRICTION FOR
A TILT-PAD THRUST BEARING WITH CROWN AND
ROUGHNESS UNDER HYDRODYNAMIC AND
MIXED LUBRICATION

by
Thomas L. Daugherty

SHIP MATERIALS ENGINEERING DEPARTMENT
RESEARCH AND DEVELOPMENT REPORT

DTIC
ELECTE
SEP 2 1 1984
B

July 1984

DTNSRDC–84/025

MAJOR DTNSRDC ORGANIZATIONAL COMPONENTS

```
                        ┌─────────────────────┐
                        │      DTNSRDC        │
                        │  COMMANDER      00  │
                        │ TECHNICAL DIRECTOR  │
                        │                 01  │
                        └─────────────────────┘
```

OFFICER-IN-CHARGE CARDEROCK 05	OFFICER-IN-CHARGE ANNAPOLIS 04
SYSTEMS DEVELOPMENT DEPARTMENT 11	
SHIP PERFORMANCE DEPARTMENT 15	AVIATION AND SURFACE EFFECTS DEPARTMENT 16
STRUCTURES DEPARTMENT 17	COMPUTATION, MATHEMATICS AND LOGISTICS DEPARTMENT 18
SHIP ACOUSTICS DEPARTMENT 19	PROPULSION AND AUXILIARY SYSTEMS DEPARTMENT 27
SHIP MATERIALS ENGINEERING DEPARTMENT 28	CENTRAL INSTRUMENTATION DEPARTMENT 29

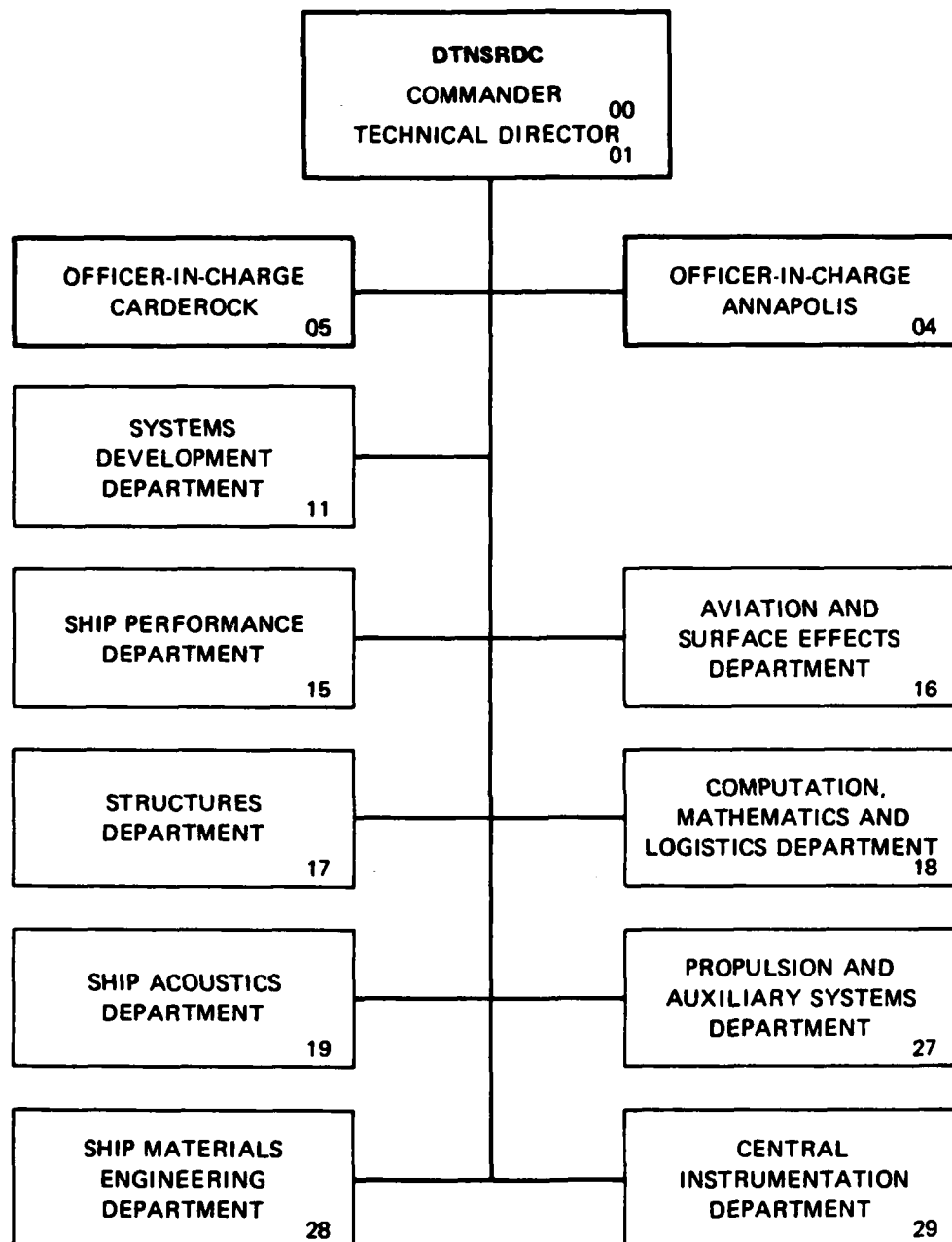| REPORT DOCUMENTATION PAGE		READ INSTRUCTIONS BEFORE COMPLETING FORM
1. REPORT NUMBER 84/025	2. GOVT ACCESSION NO. *AD-A145 752*	3. RECIPIENT'S CATALOG NUMBER
4. TITLE *(and Subtitle)* COMPARISON OF PREDICTED AND MEASURED FRICTION FOR A TILT-PAD THRUST BEARING WITH CROWN AND ROUGHNESS UNDER HYDRODYNAMIC AND MIXED LUBRICATION		5. TYPE OF REPORT & PERIOD COVERED Final
		6. PERFORMING ORG. REPORT NUMBER
7. AUTHOR(*s*) Thomas L. Daugherty		8. CONTRACT OR GRANT NUMBER(*s*)
9. PERFORMING ORGANIZATION NAME AND ADDRESS David W. Taylor Naval Ship Research & Development Center, Bethesda, MD 20084		10. PROGRAM ELEMENT, PROJECT, TASK AREA & WORK UNIT NUMBERS Program Element 61152N Task Area ZR0240301 Work Unit 2832-121
11. CONTROLLING OFFICE NAME AND ADDRESS		12. REPORT DATE July 1984
		13. NUMBER OF PAGES 52
14. MONITORING AGENCY NAME & ADDRESS*(If different from Controlling Office)*		15. SECURITY CLASS. *(of this report)* UNCLASSIFIED
		15a. DECLASSIFICATION/DOWNGRADING SCHEDULE

16. DISTRIBUTION STATEMENT *(of this Report)*

APPROVED FOR PUBLIC RELEASE; DISTRIBUTION UNLIMITED.

17. DISTRIBUTION STATEMENT *(of the abstract entered in Block 20, if different from Report)*

18. SUPPLEMENTARY NOTES

19. KEY WORDS *(Continue on reverse side if necessary and identify by block number)*

Bearings	Mixed Lubrication
Hydrodynamic	Friction
Lubrication	Thrust Bearings

20. ABSTRACT *(Continue on reverse side if necessary and identify by block number)*

In a controlled experiment on a tilt-pad thrust bearing having measured surface crown and longitudinal roughness, the frictional results were compared with results predicted by a physico-mathematical model of the bearing. The bearing operated hydrodynamically using 2190 TEP oil at

(Continued on reverse side)

DD FORM
1 JAN 73 1473   EDITION OF 1 NOV 65 IS OBSOLETE
S/N 0102-014-6601

(UNCLASSIFIED)

Block 20 continued

ambient and 150°F bulk temperature under loads approaching 500 psi. The curve of the coefficient of friction as a function of the parameter $\mu U/PB$ derived from the experiment was parallel to the curve predicted by the model under hydrodynamic conditions but the values were higher than those predicted. This difference was attributed primarily to end leakage, which was not considered in the model. A low viscosity lubricant, MIL-H-5606, was used in experiments in the transition between hydrodynamic and mixed lubrication regimes. However, this fluid exhibited non-Newtonian behavior thereby complicating comparisons with model predictions.

Because so little experimental data are available on the tribological interaction occurring with non-Newtonian fluids, additional experiments should be conducted so that a more sophisticated model can be developed of slider bearings such as the tilt-pad thrust bearing operating in the mixed lubrication regime.

Some areas in need of additional work were outlined, and experiments are needed to confirm some of the assumptions used in model analyses.

DTIC
S ELECTE D
SEP 2 1 1984
B

Accession For	
NTIS GRA&I	✓
DTIC TAB	☐
Unannounced	☐
Justification	
By	
Distribution/	
Availability Codes	
Dist	Avail and/or Special
A-1	

TABLE OF CONTENTS

LIST OF FIGURES

LIST OF TABLES

NOMENCLATURE

a	Ratio of inlet to outlet film thickness (h_1/h_2)
B	Bearing width in the direction of motion
c	Half total range of random film thickness variable
C	Constant of integration
C_p	Center of pressure
$\dfrac{d}{dx}$	First derivative with respect to x
E ( )	Expected Value of ( )
f	Coefficient of friction
F	Total applied thrust load
F_N	Normal applied force
F_R	Runner friction force
F_S	Force to shear
g(x)	Dummy function of x
h(x)	Smooth fluid film thickness as function of x
h	Smooth film thickness
h_1	Inlet film thickness to bearing
h_2	Outlet film thickness to bearing
h*	Limiting value of h used to prevent ln (h—h*) from being unbounded
h_o	Minimum film thickness for fixed inclined slider
h_s	Randomly distributed roughness height
H	Film thickness including roughness deviations
H_c	Bearing pad crown height
K	A constant
K_{fr}	Friction coefficient factor
K_p	Pressure coefficient factor

l	Length of bearing 90° to direction of motion
l_1	Distance from leading edge of bearing where pure hydrodynamic conditions exist
l_2	Distance from leading edge of bearing where mixed lubrication exists
m	Bearing inclination angle
OD	Bearing outside diameter
p	Main hydrodynamic film pressure
P_{avg}	Average bearing pressure
$\hat{P}$	Pressure within the mixed lubrication zone
P_y	Yield stress of weaker bearing material
$r(x)$	Fraction of bearing area formed by the valleys between asperity elements
R	Radius to the bearing pad center
R_c	Rockwell C hardness
R_o	Combined surface roughness
s	Shear stress of the weaker bearing material
T	Torque on test machine shaft
U	Velocity of runner surface
w	Load capacity per unit width
W	Total bearing load capacity
x	Coordinate in direction of motion
x_c	Distance from bearing inlet to film cavitation region
η	Side leakage correction factor
σ	Standard deviation
$\tau(x)$	Shear stress of slider from hydrodynamic action
$\hat{\tau}$	Shear stress on slider due to mixed lubrication
μ	Lubricant viscosity

ABSTRACT

In a controlled experiment on a tilt-pad thrust bearing
having measured surface crown and longitudinal roughness,
the frictional results were compared with results predic-
ted by a physico-mathematical model of the bearing. The
bearing operated hydrodynamically using 2190 TEP oil at
ambient and 150°F bulk temperature under loads approaching
500 psi. The curve of the coefficient of friction as a
function of the parameter $\mu U/PB$ derived from the experiment
was parallel to the curve predicted by the model under
hydrodynamic conditions but the values were higher than
those predicted. This difference was attributed primarily
to end leakage, which was not considered in the model.
A low viscosity lubricant, MIL-H-5606, was used in experi-
ments in the transition between hydrodynamic and mixed
lubrication regimes. However, this fluid exhibited non-
Newtonian behavior thereby complicating comparisons with
model predictions.

Because so little experimental data are available on
the tribological interaction occurring with non-Newtonian
fluids, additional experiments should be conducted so that
a more sophisticated model can be developed of slider
bearings such as the tilt-pad thrust bearing operating in
the mixed lubrication regime.

Some areas in need of additional work were outlined,
and experiments are needed to confirm some of the assumptions
used in model analyses.

ADMINISTRATIVE INFORMATION

BACKGROUND

A wide variety of sliding surface components used in shipboard machinery are
designed to operate with a film of lubricant between the mating surfaces. The bear-
ings on the main shafting are examples. Inboard bearings usually consist of an oil
lubricated main thrust bearing and several oil lubricated lineshaft journal bearings,
whereas outboard bearings in the U.S. Navy are lubricated with seawater and are
stave type or full molded sterntube and strut bearings. All these bearings are of
the hydrodynamic type. That is, lubricant film is established by the relative
sliding velocity between the bearing surface and the mating surface. The lubricant

film that is developed forces the two surfaces apart and thereby eliminates both
surface contact and wear. However, these bearings must operate part of their life
under conditions where there is no full lubricant film. Starts, stops, transient
operations, and operation on jacking gear are examples of some of those conditions.
If lubricant films are not thick enough to keep the surfaces apart, surface
irregularities interact and wear results.

The frictional performance of such bearings can be described by use of the
Stribeck curve[1] shown in Figure 1. Three lubrication regimes are shown-- boundary,
mixed, and hydrodynamic. The curve shows that friction is dependent upon lubricant
viscosity (μ), the relative velocity of the mating surfaces (U), and the normal
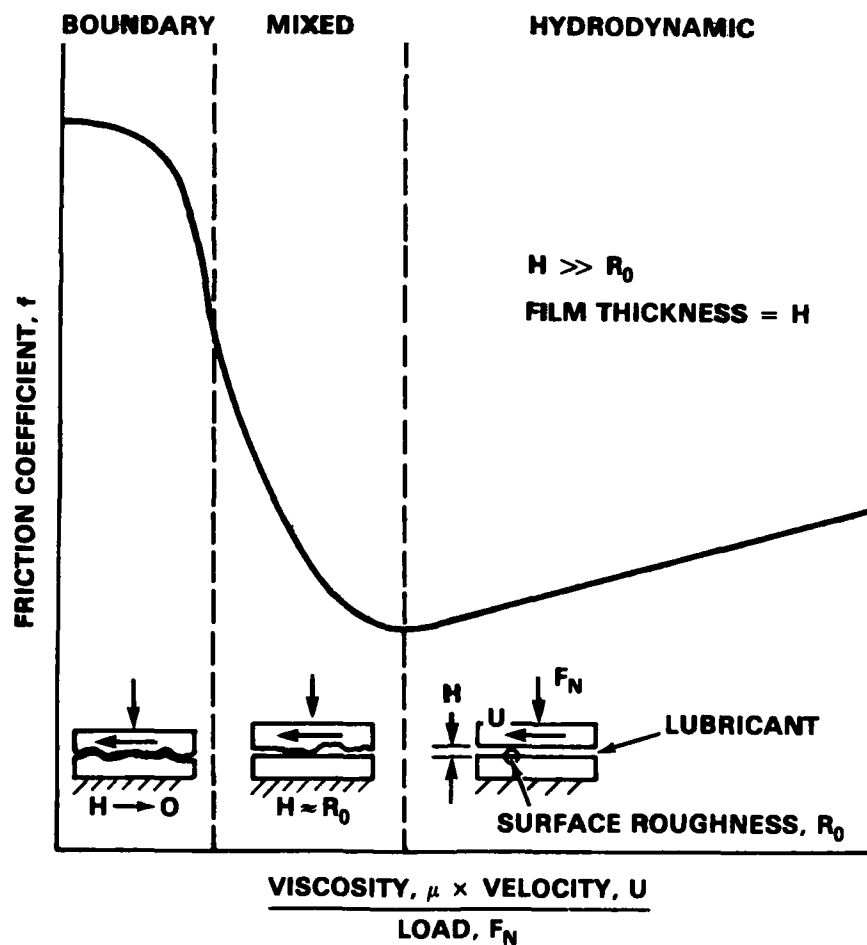force (F_N).

Figure 1 - Stribeck Curve and Lubrication Regimes

*References are listed on page 43.

2

In the hydrodynamic region, the rigid surfaces are separated by a continuous lubricant film, whose thickness, h, is much larger than the combined surface roughness, R_o. Friction is primarily due to shearing within the lubricant. This is the desirable region of operation for most bearings because there is no contact and thus no wear.

There is contact between asperities if the viscosity of the lubricant or the relative sliding velocity is reduced or if the load is increased so that the film thickness approaches the combined surface roughness, R_o. Then the load is carried by lubricant film pressure produced by hydrodynamic effects as well as by asperity contact. Under these mixed lubrication conditions, the magnitude of load carried by asperities increases with lower values of $\mu U/F_N$. Friction and wear also increase.

If $\mu U/F_N$ is such that the film thickness approaches zero, almost all the load is carried by the asperity contacts. Hydrodynamic influence is negligible and wear is governed more by the physico-chemical properties of the lubricant and the mating surface and their interaction.

Design charts have been developed for frequently used bearings such as the tilt-pad slider bearing.[2] Operating characteristics of the tilt-pad bearing depend on the pivot position and the profile of the pad surface and can be optimized by the proper selection of pivot and profile. The tilt-pad thrust bearing the U.S. Navy uses for the main propulsion shafting is pivoted in the center of the pad, thereby allowing good (not optimum) operation in either direction. According to simple theory using the Reynolds equation, a centrally pivoted pad with a flat surface has no load capacity.[2] However, experience has shown that centrally pivoted pads perform reasonably successfully. Load capacity of a centrally pivoted tilt-pad bearing can be predicted adequately by considering effects of pad crown,[3] of variable lubricant viscosity as the lubricant passes between the bearing and the mating surface, and of variable lubricant density.

Crowning of the pad surface has a strong influence on improving the performance of the centrally pivoted tilt-pad bearing. Some degree of crowning is expected on new bearings, but most results from deformations caused by the oil film pressure distribution and thermal gradient across the pad thickness during operation. However, an excessive crown may produce poor performance.

OBJECTIVE

Although the frictional performance of tilt-pad bearings operated in the hydro-dynamic lubrication regime can be predicted by theoretical consideration, the literature contains little experimental evidence of performance in the transition region between hydrodynamic and mixed lubrication conditions. Thus, the goal of the project was to develop a model for sliding surface bearings that would extend the hydrodynamic theory continuously into the mixed lubrication region. This report compares the frictional results from a controlled experiment on a tilt-pad thrust bearing having measured surface and longitudinal roughness with the predictive results from a model of the bearing.

APPROACH

A set of centrally pivoted tilt-pad thrust bearings was obtained commercially. The pads were crowned to simulate thermal and elastic pad distortions and roughened in a longitudinal direction to simulate expected roughness patterns generated during operation. The topography of each pad and mating runner surface was measured and the surface characterized by crown height and a roughness magnitude. These values and bearing and material description, speed, and lubricant characteristics were used in a computer program of a model of the bearing. The theory and the model are described below.

The predicted frictional behavior of each pad and of the complete bearing were obtained from the computer program. The resulting friction coefficient was plotted against the parameter in $\mu U/PB$ to form a plot similar to the Stribeck curve shown in Figure 1. A friction curve resulted showing a prediction of performance in the hydrodynamic region of operation and into the mixed lubrication region. Other meaningful outputs, such as the minimum film thickness, inlet to exit film thickness ratio and location of mixed lubrication zone, were also generated by the computer program.

Next a series of experiments was conducted on the set of modified thrust bearings over a range of $\mu U/PB$ values and the frictional torque recorded. The coefficients of friction were computed for the values of $\mu U/PB$ and compared with the predicted results.

THEORETICAL BASIS FOR THE MODEL

The model for mixed and hydrodynamic lubrication of a crowned tilt-pad thrust bearing with longitudinal roughness, which was developed under this project, is an extension of an earlier analysis of a fixed inclined bearing with longitudinal roughness.[4] The bearing pad is free to pivot until a moment equilibrium position is attained. The model geometry is shown in Figure 2. The pad surface is crowned, with the maximum pad height at the center. The film thickness due to the crowning, the angle of inclination, the ratio of inlet to outlet film thickness, and the pad geometry can be expressed as:

$$h(x)=h_2 \ \{a + (1-a)[(1 + 4 \ H_c/mB)\left(^x/B\right) - (4 \ H_c/mB)\left(\frac{x}{B}\right)^2]\}$$

The expression is for a smooth surface and is a function of the x coordinate. Another term must be added when roughness is being considered. A film height would then consist of:

$$H = h(x) + h_s$$

where h_s is the randomly distributed roughness term.
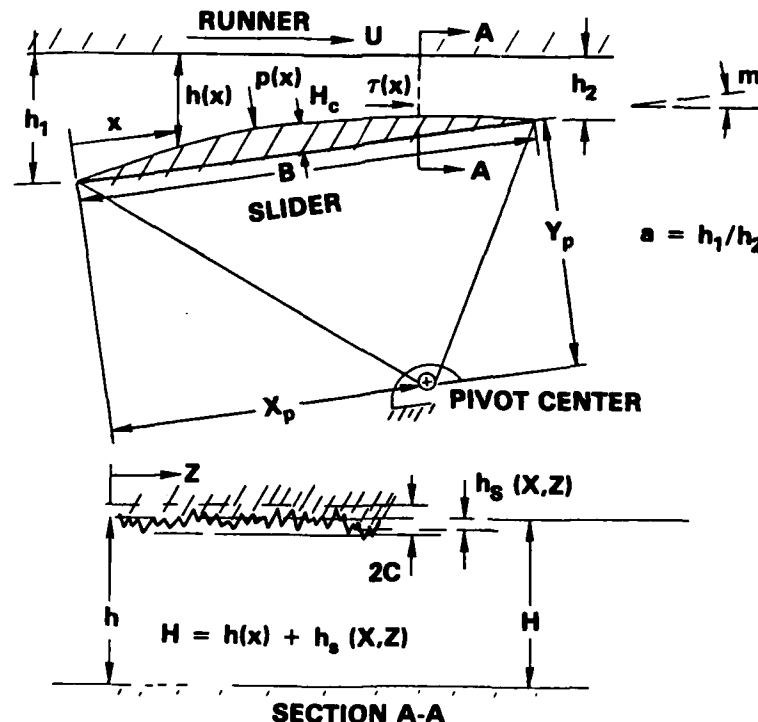
Figure 2 - Curved Slider Bearing with Surface Roughness (from Daugherty and Pan[5])

Experimental evidence indicates that many engineering surfaces have a distribution of random heights that is very nearly Gaussian, at least within three standard deviations. We used Christensen's polynomial distribution function to approximate the Gaussian distribution.[4]

$$f(h_s) = \frac{35}{32c^7}(c^2 - h_s^2)^3, \quad -c \leq h_s \leq c$$

$$= 0 \text{ elsewhere}$$

where $2c$ is the domain of the function. The function becomes zero at $c=3\sigma$, where σ is the standard deviation. The above equation will be considered a description of the combined roughness when both the bearing and runner surfaces are rough

The following assumptions were made:

- Lubricant viscosity is constant.
- Lubricant density is constant.
- Reynolds' equation holds for hydrodynamic and mixed lubrication conditions.
- There is no side leakage.
- No effects are caused by material/lubricant interactions of a chemical-physical nature.
- Centrifugal effects are negligible.
- Lubricant is Newtonian.
- Film pressure does not vary across film.

The basic form of Reynolds' equation under steady state conditions is

$$\frac{d}{dx}\left[E(H^3)\frac{dp}{dx}\right] = 6\mu U \frac{d}{dx}E(H)$$

Where $E(\ )$ is the expected value of $(\ )$, and $H = h(x) + h_s$. The quantity p is the mean hydrodynamic pressure at any location x, U is the slider speed, and μ is the lubricant viscosity. The expectancy operator is defined as:

$$E[g(x)] = \int g(x)f(h_s)dh_s,$$

where the upper limit of integration is always c, and the lower limit $-c$ or $-h$, depending upon whether the film thickness is greater or less than c. This corresponds to regions of pure hydrodynamic and mixed lubrication. In regimes of pure hydrodynamic lubrication, it can be shown that:

$$E(K) = K, \text{ a constant}$$

$$E(H) = h,$$

$$\text{and } E(H^3) = h^3 + h\, c^2/3$$

Under mixed lubrication conditions these parameters are much more complicated:

$$E(K) = K/32c^7) \left| 16c^7 + 35c^6h - 35c^4h^3 + 21c^2h^5 - 5h^7 \right|$$

$$E(H) = 35/32c^7) \left| \frac{c^8}{8} + \frac{16c^7h}{35} + \frac{1c^6h^2}{2} - \frac{1c^4h^4}{4} + \frac{1c^2h^6}{10} - \frac{1h^8}{56} \right|$$

and

$$E(H^3)=35/32c^7 \left| \frac{1c^{10}}{40} + \frac{16c^9h}{105} + \frac{3c^8h^2}{8} + \frac{16c^7h^3}{35} + \frac{1c^6h^4}{4} - \frac{1c^4h^6}{20} + \frac{3}{280}c^2h^6 - \frac{1}{840}h^{10} \right|$$

The pressure distribution within the lubricant film can be determined by integrating Reynolds' equation. The first integration yields:

$$\frac{dp}{dx} = 6\mu U \left[(E(H)/E(H^3)) + C/E(H^3) \right]$$

where C is a constant of integration.

The second integration yields:

$$p = 6\mu U \int_0^x (E(H)/E(H^3))dx + C\int_0^x \left(\frac{1}{E(H^3)} \right) dx$$

The boundary conditions are $p(o) = p(B) = 0$. The constant of integration is:

$$C = - \int_0^B (E(H)/E(H^3))dx / \int_0^B \left(\frac{1}{E(H^3)} \right) dx$$

In the mixed lubrication region, the metallic contact load is assumed equal to the product of the yield stress of the weaker bearing material and the fraction of area, per unit bearing width, over which such contact takes place. The load capacity per unit width can therefore be expressed as:

$$w = \int_0^{l_1} pdx + \int_{l_1}^{l_2} \hat{p}dx + \int_{l_2}^B pdx$$

where p is the ordinary hydrodynamic pressure upstream and downstream of the area of asperity interactions and $\hat{p}$ is the pressure in the mixed lubrication zone. These regions are shown visually in Figure 3. In the first region from $x=0$ to $x=l_1$, the film thickness exceeds the critical film thickness and converges in the direction of motion. Significant load carrying hydrodynamic pressure is generated in the lubricant film. In the region from $x=l_1$ to $x=l_2$ the film thickness is less than the critical film thickness, producing mixed lubrication. Load support is generated by a combination of asperity contact and hydrodynamic pressure between asperity interactions. In this region the smooth film thickness goes through a converging and then a diverging region. In the remaining region from $x=l_2$ to $x=B$ the film thickness again exceeds the critical film thickness, thereby signifying that there are no asperity interactions. The pressure produced in this region results from hydrodynamic action only. The film thickness diverges in the direction of motion; therefore no load support is generated in this region.

Load carried by the second region is supported in part by the hydrodynamic pressures generated between the asperities that are in contact and in part by the asperity loads themselves as follows:

$$\int_{l_1}^{l_2} \hat{p} dx = \int_{l_1}^{l_2} r(x) p dx + p_y \int_{l_1}^{l_2} (1-r) dx$$

where p_y is the yield stress of the weaker bearing material and r is the fraction of bearing area formed by the valleys between asperity elements

$$r = \frac{1}{32c^7} \left\{ 16c^7 + 35c^6h - 35c^4h^3 + 21c^2h^5 - 5h^7 \right\}$$

per unit bearing width.

The center of pressure can be obtained by the following formula:

$$C_p = \int_0^B p x dx / \int_0^B p dx$$

The center of pressure is used to obtain moment balance of the thrust pad about its center of pressure by equating the product of the load and the center of pressure distance from the pivot point to the product of the friction on the pad surface and its distance to the center of pivot.

The shear stress acting on the slider surface from hydrodynamic action is given by:

8

$$\tau(x) = \mu UE(1/H) + \frac{1}{2}\left(\frac{dp}{dx}\right)E(H)$$

The total friction force can be determined in a similar manner to the load capacity. That is,

$$F_s = \int_0^{l_1} \tau\,dx + \int_{l_1}^{l_2} \hat{\tau}\,dx + \int_{l_2}^{B} \tau\,dx$$

where $\int_{l_1}^{l_2} \hat{\tau}\,dx = \int_{l_1}^{l_2} r\tau\,dx + s\int_{l_1}^{l_2}(1-r)dx$

where s is the shear stress of the weaker bearing material.

The expectation value $E(1/H)$ must be evaluated for the hydrodynamic and mixed regions to determine the friction force –

$$E\left(\frac{1}{H}\right) = \frac{35}{32c^7}\left[(c^2 - h^2)^3 \ln\left|\frac{(h+c)}{(h-c)}\right| + \frac{2}{15}ch(15h^4 - 40c^2h^2 + 33c^4)\right]$$

for the hydrodynamic region and:

$$E\left(\frac{1}{H}\right) = \frac{35}{32c^7}\left[(c^2 - h^2)^3 \ln\left|\frac{(h+c)}{(h-h^*)}\right| + \frac{8h^3(h+c)^3}{3} - \frac{1}{6}(h+c)^6\right]$$

$$- 4(c^2 - h^2)h(h+c)^3 + 6(c^2 - h^2)^2h(h+c) + 6(c^2 - h^2)h^2(c+h)^2 - 3h^2(c+h)^4$$

$$+ \frac{6h(h+c)^5}{5} + \frac{3}{4}(c^2 - h^2)(h+c)^4 - \frac{3(c^2 - h^2)(h+c)^2}{2}]$$
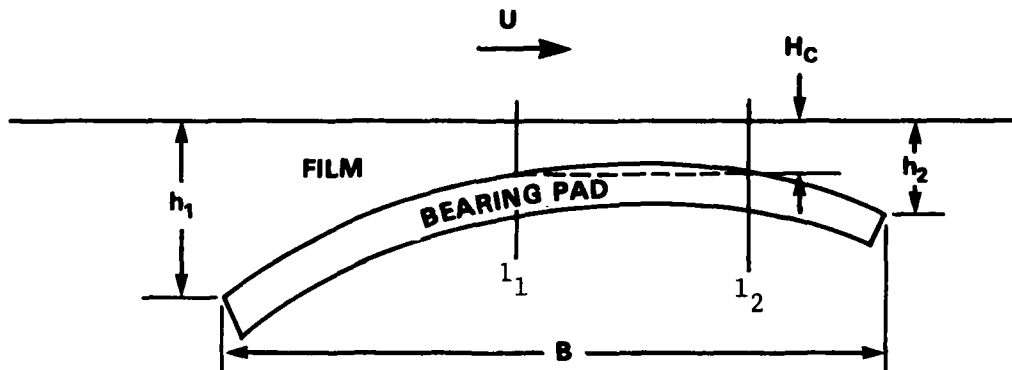
for the mixed region.

Figure 3 – Crowned Bearing Surface with Regions
of Hydrodynamic and Mixed Lubrication

9

The term h* is needed to prevent the logarithmic term from being unbounded; h* was set eoual to h-mB/1000. Numerical analysis showed that the resulting solutions were not particularly sensitive to this assumption.

The coefficient of friction may be determined by dividing the friction force by the applied load. The friction force is approximated as the sum of the friction forces (as determined in the foregoing paragraphs) and the component of load acting in the plane of rotation or:

$$F_R = F_S + mW \text{ where } F_R \text{ is the force on the runner.}$$

The friction coefficient, f, is then:

$$f = \frac{F_R}{W} = \frac{F_S}{W} + m$$

The inputs to the computer program include the rotational speed, the pad length, the viscosity of the lubricant, the mean bearing surface diameter, the roughness asperity height, the bearing material yield strength, the ratio of the shear stress to yield stress, the crown height, and the pivot coordinates.

The computer program is written in BASIC for an interactive system. It calculates a reasonable first approximation of h_1/h_2. Reynolds' equation is then successively integrated to obtain the friction and pressure moments. If the moment is greater than the product of the load and one-tenth of one percent of the bearing length, then a new value of h_1/h_2, calculated from a "hunting" routine, is inserted, and the process is repeated until the moment balance criterion is met.

When the moment balance criterion has been met, the operator receives a list of pertinent bearing parameters such as load and friction forces broken down into contributions from pure hydrodynamic, mixed, and asperity contact forces; shear and pressure moments; the center of pressure; coefficient of friction; value of $\mu U/PB$; h_1/h_2 ratio; and the minimum film thickness and its location. The operator can choose additional conditions and rerun.

The initial computer program was developed by Dr. B. Carson under Navy Contract N00600-78-D-1302 (HW-22) with CADCOM, a division of Mantech International Corporation. That program was modified to improve the iteration scheme used (which reduced computer time and improved the search portion); to obtain a pressure plot of the film within the bearing; and to determine effects of cavitation in the diverging region of the film. In the original program, significant negative

10

pressures were predicted using Reynolds' equation and boundary conditions of
$p(0) = p(B) = 0$. A diverging film was formed when the trailing edge was not the
location of minimum film thickness. It is generally believed that a subambient
pressure condition in the fluid cannot be sustained;[6,7] instead, the film ruptures
or cavitates somewhere so that the ambient condition will be reached internally
with a vanishing pressure gradient. This is the Reynolds-Swift-Stieber condition
of film rupture or cavitation and is stated as:

$$p(x_c) = 0$$

$$\left. \frac{dp}{dx} \right|_{x_c} = 0$$

$$0 < x_c < B$$

where x_c is the location of the cavitation or rupture boundary.

EXPERIMENTAL MATERIALS

TEST MACHINE

Figure 4a is a photograph of the machine we used to measure friction on crowned
tilt-pad bearings having a longitudinal roughness pattern. The machine has six
main parts—hydraulic motor, reduction gear, torque sensor, oil tank, load blocks,
and heater. The test bearing (Figure 4b) is located in the oil tank section. A
schematic of the test machine is shown in Figure 5. The shaft is vertical and is
positioned with ball bearings. An octagonal bearing with a series of linear bear-
ings on each face allows the runner to move axially while transmitting torque
(Figure 6). Two sets of three tilt-pad bearings are mounted on a metal ring and are
submerged in the lubricant. The oil reservoir contains 7-1/2 quarts of lubricant
and the frame is made of plexiglass to allow viewing during operation. Two steel
plates are attached to the runner as mating surfaces to the bearings. The lubricant
can be heated by circulating hot water through coils.

11

1 HYDRAULIC MOTOR   4 OIL TANK
2 REDUCTION GEAR   5 LOAD PISTON BLOCKS
3 TORQUE SENSOR   6 HEATER

FIGURE 4a — TEST MACHINE

1 HEATING COIL   3 TEST BEARING
2 RUNNER PLATES   4 THERMOCOUPLE
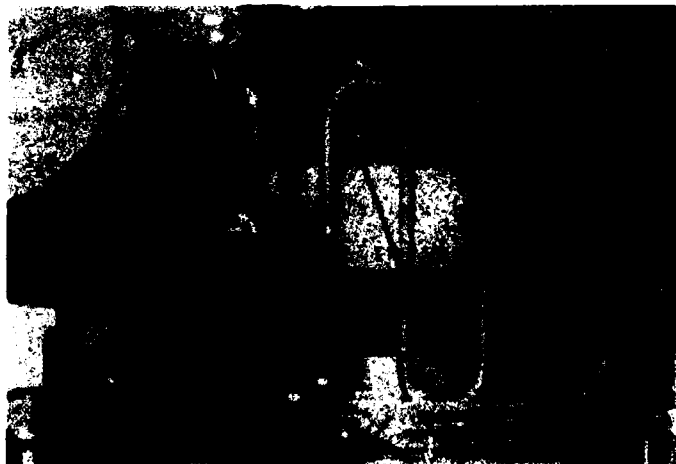
FIGURE 4b — TEST BEARING IN OIL TANK

Figure 4 – Test Machine Used To Conduct
Friction Measurements
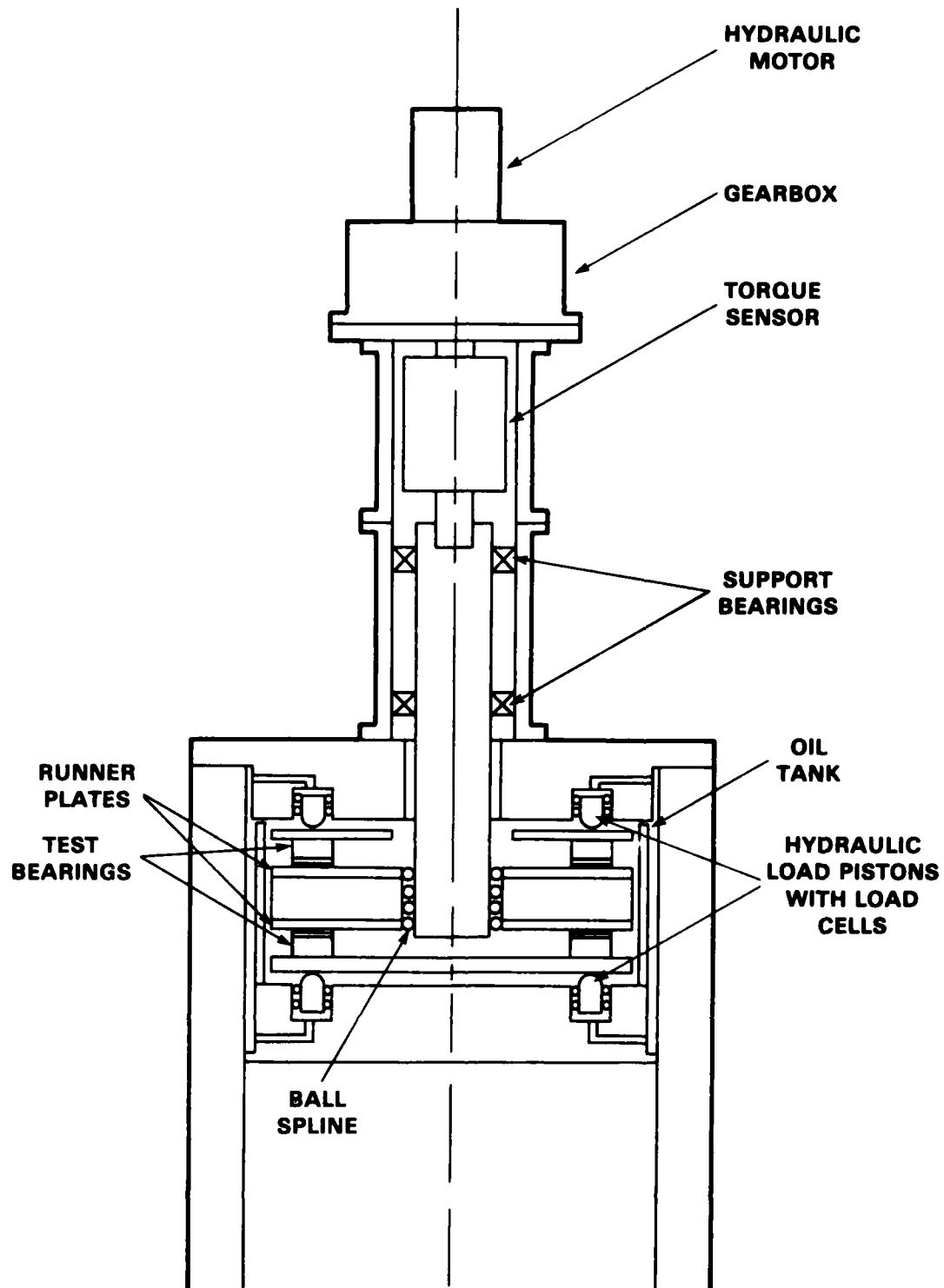
Figure 5 - Test Machine Schematic

Figure 6 – Thrust Runner Showing Octagonal Bearing
and Mating Surface for Top Set of Bearings

The rotational speed is set at a nominal 35 rpm. A hydraulic load is applied
to the upper set of bearings and transmitted through film to the runner, back
through the film of the lower bearing set and through the lower set to the test
machine frame. The thrust load is carried by only the two sets of test bearings.
This allows accurate measurements of friction in test bearings because support
bearings cause little torque. The parameters measured are speed, torque, load, and
bulk oil temperatures. The thrust runners are of 1040 steel (50 R_c Hardness). They
are machined to produce circumferential machining marks, which represent the desired
longitudinal roughness pattern. Roughness measurements are described in the section
on topographic analysis below. The thrust runner is shown in Figure 6.

Load is applied by supplying hydraulic pressure to three pistons located in the
top load block. Each piston is located directly over the thrust bearings. A load
cell in each piston monitors the applied load.

14

DESCRIPTION OF THE TEST BEARINGS

The bearing we used in these experiments is a commercially available, three shoe element tilt-pad thrust bearing made by Kingsbury Machine Works, Inc., as bearing number NN-7. The shoes or pads are equally spaced about the shaft with 120° between pad centers. The three pad arrangement shown in Figure 7 is mounted on a leveling washer which allows loads to be distributed among the three pads. The bearing inside diameter is 3.5 in. and the outside diameter is 7 in. The net area of the three pads is 12.3 in.^{2} Each pad is fabricated of steel, is about 3/4-in. thick and has a 1/16-in. thick babbitt surface (ASTM B23) and a hardened steel insert in the backing (see Figure 8). The hardened steel insert has a spherical surface, which allows the shoe to pivot and form a load-carrying lubricant film between the shoe's babbitt surface and the runner surface. The two sets of thrust pads were positioned so that the pads from one set were located directly opposite the other set. Figure 9 shows the bearing arrangement with the top load ring, top set of pads, top runner surface, runner, bottom runner surface, bottom set of pads, and bottom load ring. Three load pistons, one over each of the top pads, apply a hydraulic load to the bearing.

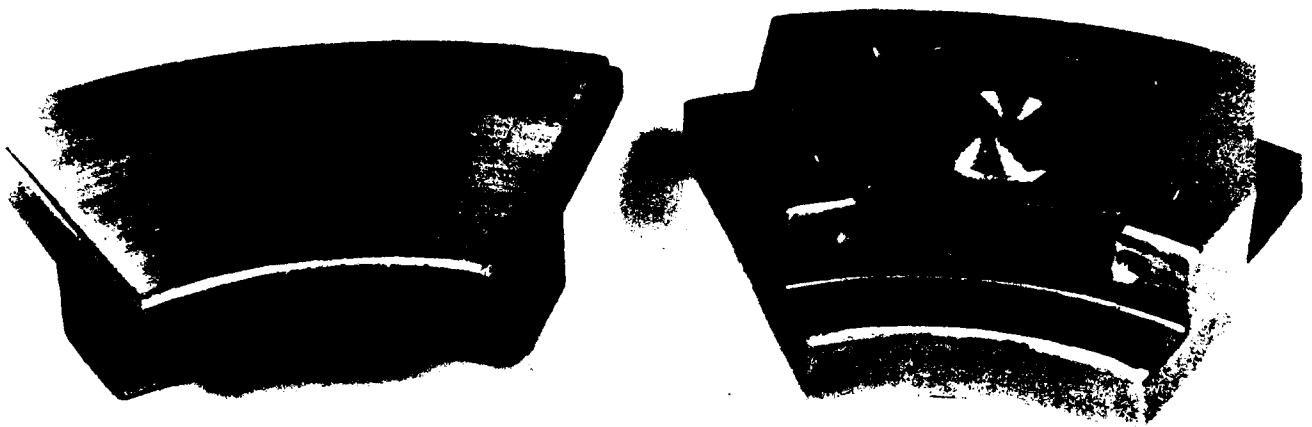Figure 7 – Three-Pad Thrust Bearing Mounted on Leveling Washer

Figure 8 - Front and Back Surfaces of Tilt-Pad Bearing

1 SHOE (BABBITT FACED)
2 SHOE SUPPORT (IN SHOE)
3 SHOE CAGE
4 SHOE CAGE PLUG
5 SHOE CAGE KEY
6 SHOE CAGE KEY SCREW
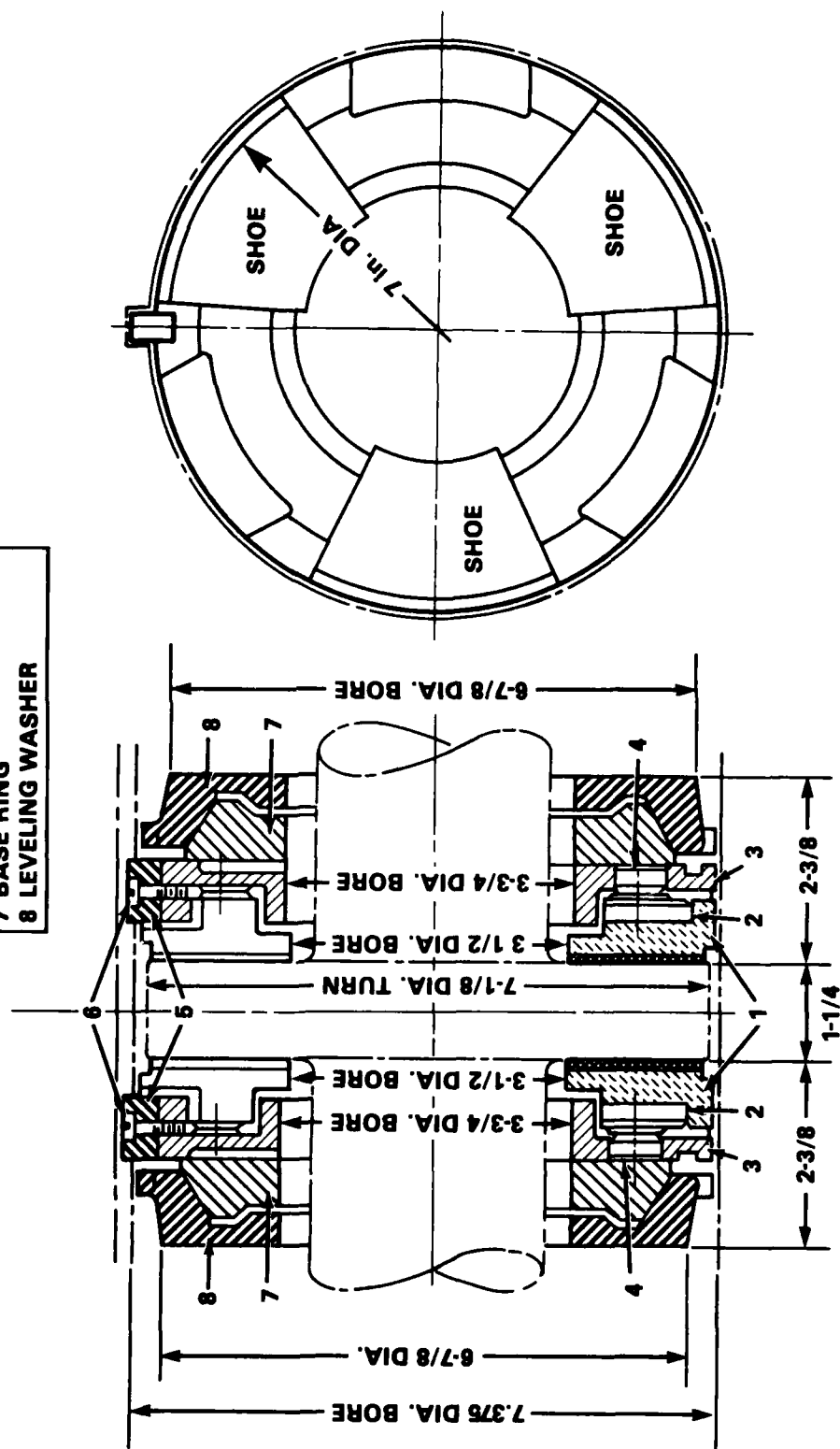**7** BASE RING
8 LEVELING WASHER

Figure 9 – Thrust Bearing Assembly Drawing

17

The crowning and longitudinal roughness on the bearing surfaces were obtained in the following manner:

- The thrust pads were installed in their respective load ring as though ready to run.
- The assembly was placed with the bearing surface down on a flat circular disc covered with emery paper.
- The disc was rotated while maintaining light pressure on assembly. The assembly was held stationary.
- Water was used on the emery paper.
- The disc was rotated in both directions until the entire surface contacted the paper, yielding a bright babbitt surface.
- Each thrust pad was then measured to determine the curvatures and roughness.

TOPOGRAPHICAL ANALYSIS OF THE TEST BEARINGS

The surface profiles and roughness of all bearing babbitt surfaces and thrust runners were obtained using the Talysurf 10 machine manufactured by Rank Taylor Hobson. It was used without a skid device so that profile data could be obtained. Figure 10 shows the standardized grid network set up for the bearing and thrust plates. Profile traces were recorded for each grid line. Five traces were taken on each bearing pad, and four traces were taken on each thrust runner. The trace lengths for the thrust pad were approximately 32 and 50 mm for the I and O traces and 30 mm for the L, C, and R traces (See Figure 10). All runner traces were about 50 mm. The profiles of the surfaces were recorded using magnification of 10,000X in the vertical direction and magnification of 2, 10, and 100X in the horizontal direction. Sample traces are shown in Figures 11 and 12 for the thrust pad and runner, respectively. The date and time, the horizontal and vertical magnification, part identification, measurement location, and the start and stop location were recorded on each trace.

Then, the R_A values over the lengths of each grid were recorded. The separate values were recorded for each line on the thrust runner and five each on the thrust pad. Different sections of the surface were sampled for the different values.

18
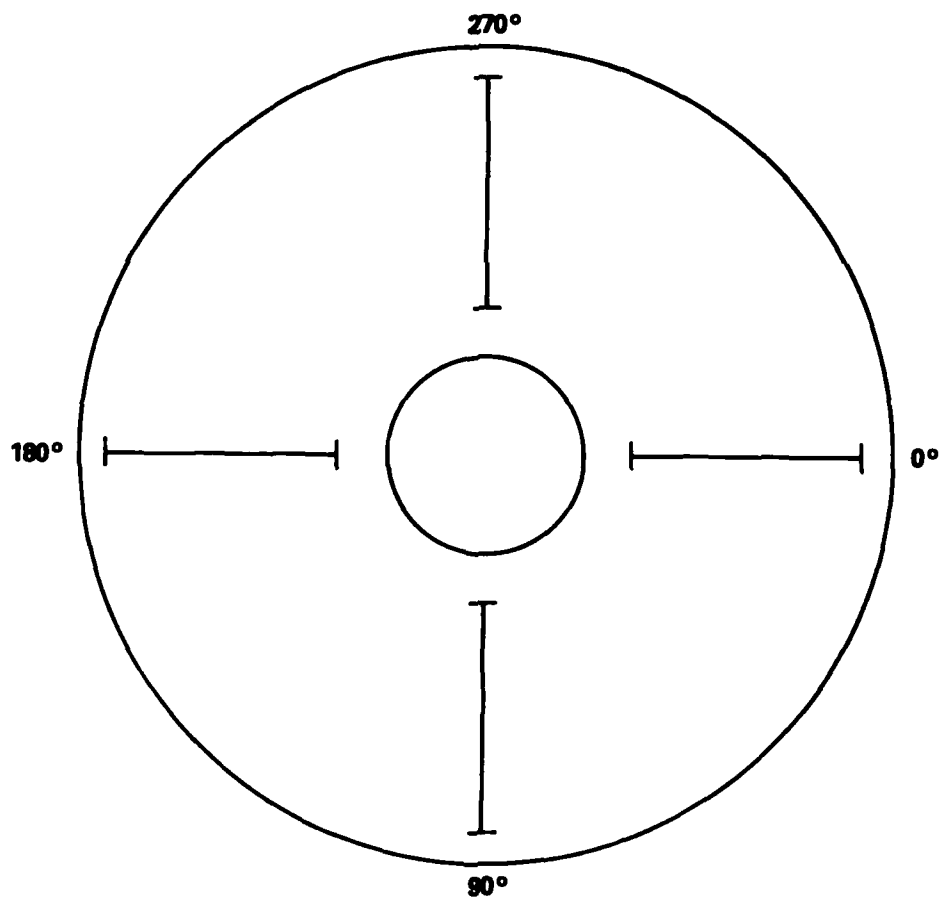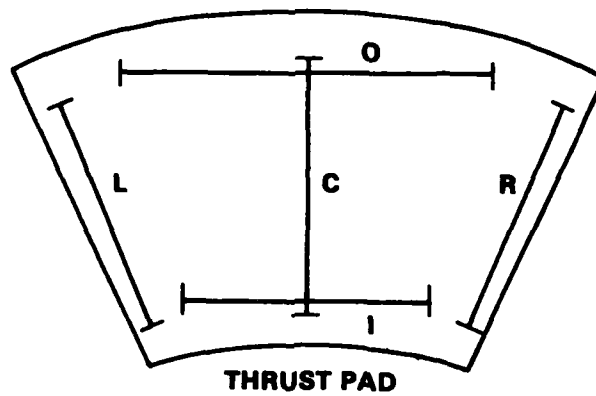
Figure 10 - Grids for Topographical Measurements of Thrust
Pads and Runner Surfaces
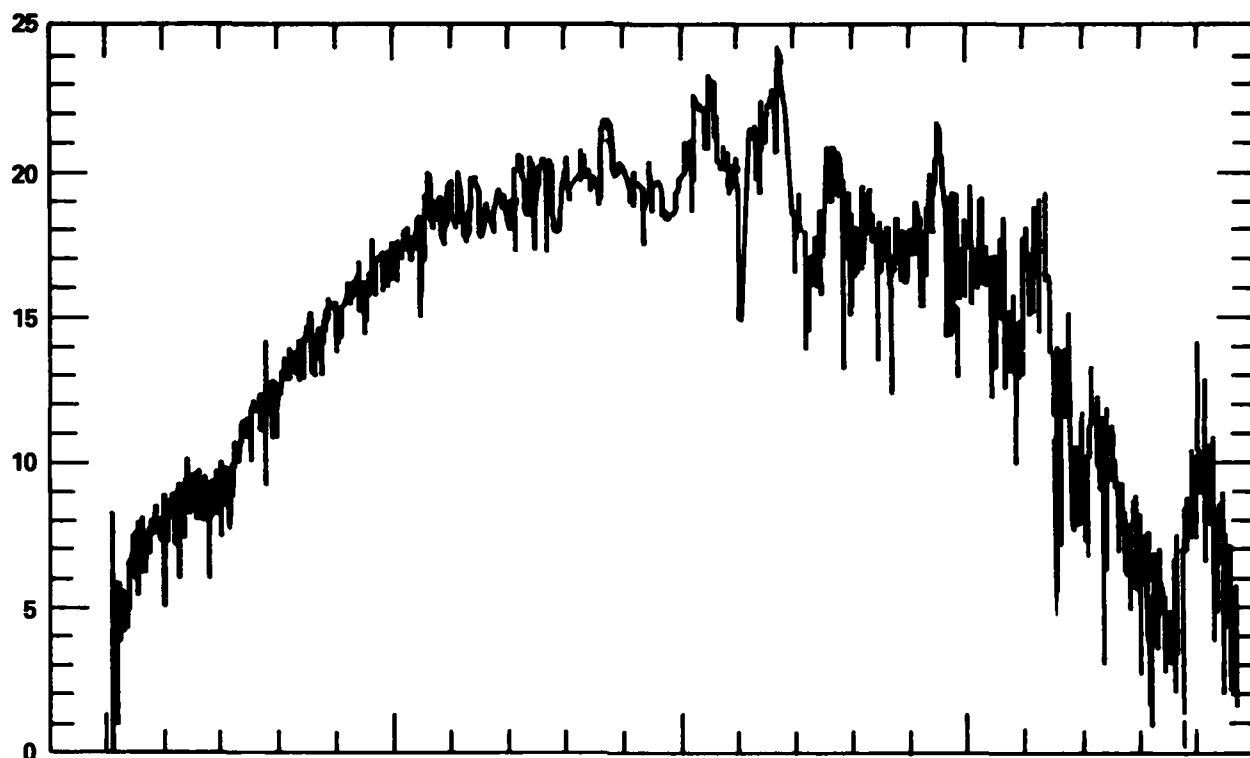
Figure 11 - Thrust Pad Talysurf Traces at 10,000× for Vertical and 2× Horizontal
Magnification for Bearing T-2, Outside Axial Trace
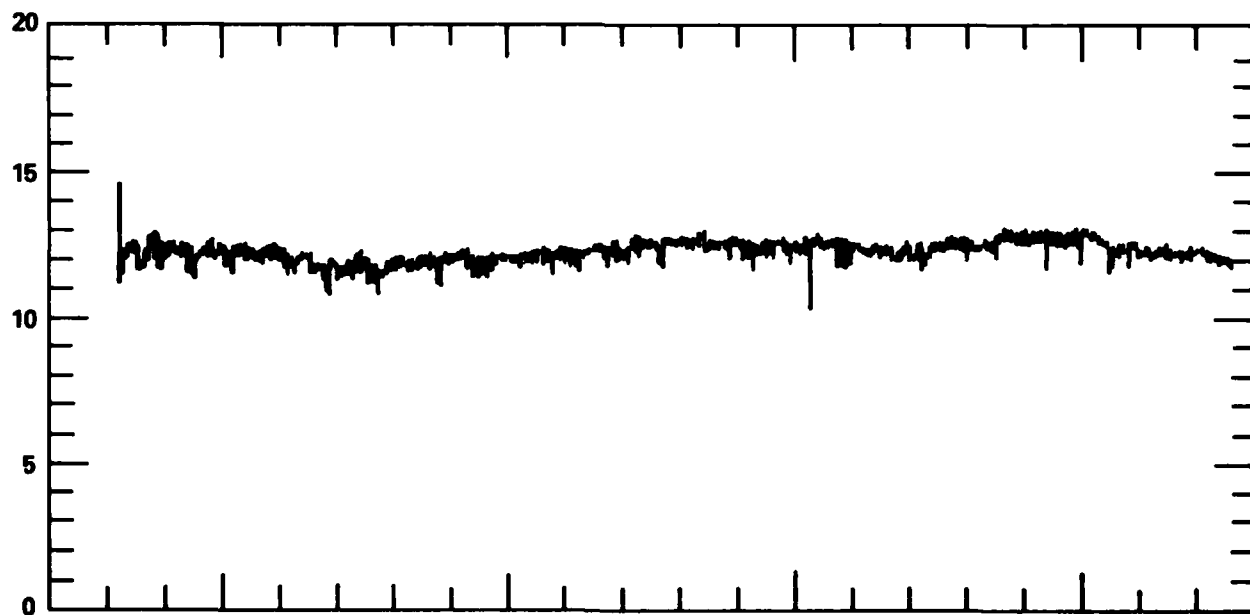
Figure 12 - Thrust Runner Talysurf Traces at 10,000× Vertical and 2× Horizontal
Magnification for Thrust Runner A at 270° Position

Each Talysurf 10 trace was characterized by the following parameters: crown height, maximum peak to valley height, and estimated peak to valley asperity representative of surface. Figure 13 shows the basis on which these parameters were evaluated. These values were tabulated for each trace in addition to the average R_A reading, the minimum R_A, and maximum R_A readings for each. The data for the bearing pad (Tables 1 and 2) and for the thrust collars (Table 3) were used to generate input to the computer program. The crown height in the direction of motion was obtained for each thrust pad by taking the maximum value recorded for either trace I or O in Figure 10. The surfaces of the thrust runner were assumed to be flat.

The radial traces on the thrust shoes and runners were used to determine the asperity height magnitude as follows: The maximum 2c values for the traces on the two runner surfaces and the thrust pads were obtained from Tables 1, 2, and 3. The resulting 2c value for each is shown in Table 4. The set of three thrust pads identified with letter "T" were mated with thrust collar A; the pads marked B were paired with thrust collar B. A composite asperity height was determined by averaging the particular pad and the mating runner. The resulting asperity height, 2c, and the crown height used in the computer program are shown in Table 5.
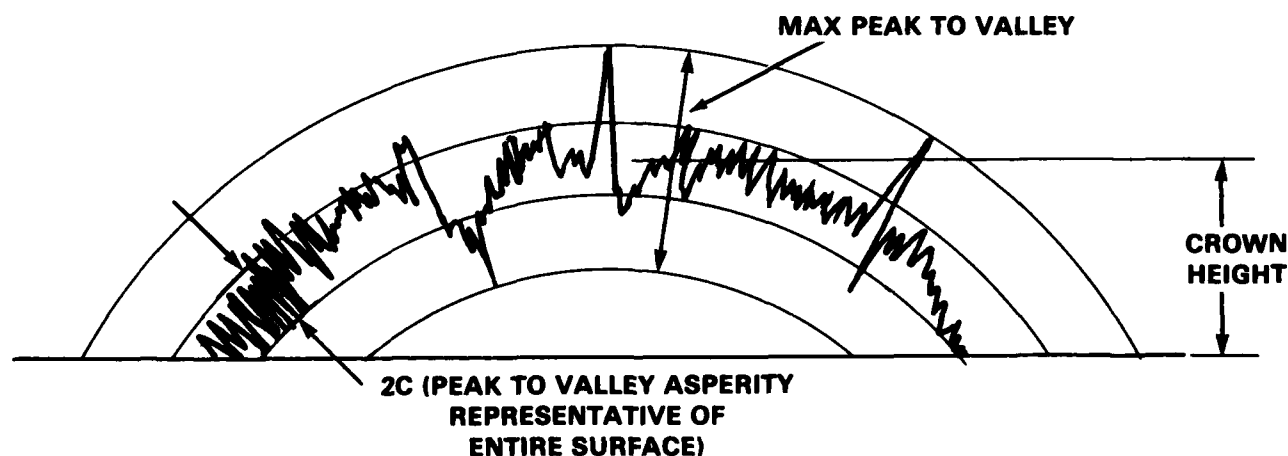
Figure 13 – Characterization of Bearing Surface Traces on Talysurf 10

21

TABLE 1 – ROUGHNESS AND CROWN MEASUREMENTS FOR BOTTOM
SET OF THRUST PADS ON A TILT PAD BEARING

Bearing No.	Location*	R_A**	R_AMin	R_AMax	Max P to P***	2c***	Axial Crown†	Radial Crown†
B-1	R	12.4	10.1	17.9	430	30	–	–100
B-1	C	13.0	11.0	16.8	150	40	–	–160
B-1	L	21.8	20.5	22.9	190	50	–	–160
B-1	I	–	–	–	240	45	+60	–
B-1	O	–	–	–	165	50	+50	–
B-2	R	13.7	10.5	20.0	130	30	–	–80
B-2	C	11.3	9.4	12.5	130	35	–	–100
B-2	L	15.7	13.8	17.9	190	50	–	–150
B-2	I	–	–	–	200	45	+75	–
B-2	O	–	–	–	350	40	–50	–
B-3	R	16.9	12.5	24.0	200	50	–	–130
B-3	C	15.2	13.9	17.5	150	40	–	–130
B-3	L	30.5	28.5	33.0	600	45	–	+70
B-3	I	–	–	–	450	40	+280	–
B-3	O	–	–	–	310	60	+550	–

*See figure 10 for location positions
**Average of five readings across surface

*** 2c ... Max Peak to Peak (P to P)

†Plus indicates a convex profile; minus indicates a concave profile.

22
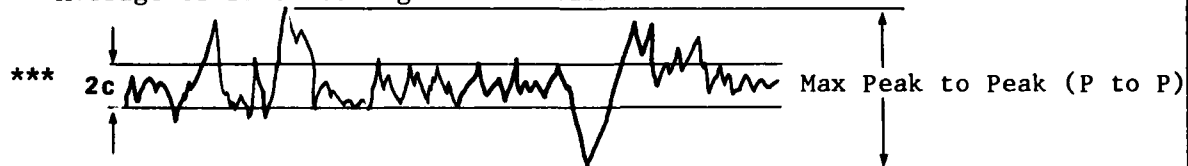
TABLE 2 – ROUGHNESS AND CROWN MEASUREMENTS FOR TOP SET
OF THRUST PADS ON A TILT PAD BEARING

Bearing No.	Location[*]	R_A[**]	R_AMin	R_AMax	Max P to P[***]	2c[***]	Axial Crown[†]	Radial Crown[†]
T-1	R	10.9	8.2	13.3	200	20	–	+150
T-1	C	16.7	9.0	20.0	550	40	–	+100
T-1	L	30.4	18.0	73.0	1150	60	–	+100
T-1	I	–	–	–	700	40	+160	–
T-1	O	–	–	–	250	20	+200	–
T-2	R	10.7	9.2	14.0	180	25	–	+70
T-2	C	11.6	7.0	14.5	300	25	–	+200
T-2	L	16.5	12.2	23.5	650	40	–	+320
T-2	I	–	–	–	125	30	+80	–
T-2	O	–	–	–	180	25	+160	–
T-3	R	18.1	13.9	21.0	150	40	–	+80
T-3	C	18.0	12.8	22.0	180	35	–	+40
T-3	L	18.8	17.3	20.0	130	45	–	+20
T-3	I	–	–	–	170	55	+80	–
T-3	O	–	–	–	170	25	+80	–

[*]See figure 10 for location positions
[**]Average of five readings across surface

[***] ... Max Peak to Peak (P to P)
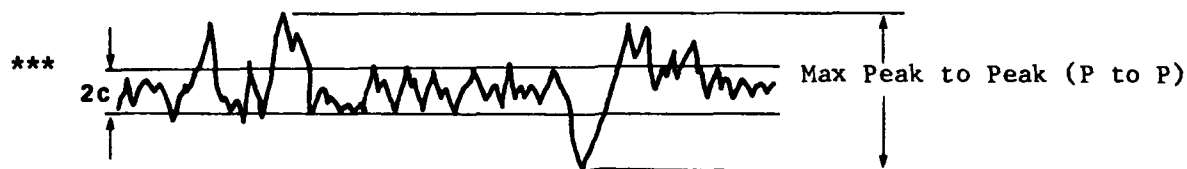
[†]Plus indicates a convex profile; minus indicates a concave profile.

TABLE 3 - ROUGHNESS AND CROWN OF THRUST COLLARS

Thrust Collar No.	Location	R_A *	R_AMin	R_AMax	Max P to P **	2c **	Radial Crown†
A-1	0°	3.2	2.5	5.5	40	10	+40
A-1	90°	2.6	2.0	3.1	30	5	-20
A-1	180°	2.5	2.1	2.9	50	5	-40
A-1	270°	2.8	2.3	3.7	30	5	+10
B-1	0°	9.5	8.2	10.3	90	25	+20
B-1	90°	9.6	8.7	11.5	150	20	+40
B-1	180°	9.2	7.2	10.7	80	20	-30
B-1	270°	8.9	8.0	9.8	90	20	+30

*Average of five readings across surface.

** 2c   Max Peak to Peak (P to P)

†Plus indicates a convex profile; minus indicates a concave profile.

TABLE 4 - MAXIMUM RECORDED 2c
VALUES FOR THE THRUST RUNNER
AND BEARING SURFACES

Thrust Runner	Maximum 2c
A-1	10
B-1	25
Bearing Number	Maximum 2c
T-1	60
T-2	40
T-3	45
B-1	50
B-2	50
B-3	50

TABLE 5 - COMPUTER INPUT BASED ON
TOPOGRAPHY OF SURFACES

Bearing No.	Crown	2c
T-1	200	35
T-2	160	25
T-3	80	27.5
B-1	60	37.5
B-2	75	37.5
B-3	550	37.5

COMPUTER ANALYSIS

The program described in the section on theory was run using the data from the topographical analysis presented in Table 5. The following input data concerning the lubricant, materials, and test conditions were used:

Rotational shaft speed   =   35 rpm

Bearing mean diameter   = $\dfrac{(\text{Bore} + \text{OD})}{2}$ = 5.2 in.

Lubricant Viscosity   = 6×10^{-6} Reyns

Shoe Length   =   2.31 in.

Asperity Height   =   value from Table 5

Yield Stress   =   9000 psi

Shear/Yield   =   0.2

Crown Height   =   value from Table 5

Pivot Center   =   0.5, 0.32

Typical output for operation in the hydrodynamic region is shown in Figure 14 and for mixed lubrication conditions in Figure 15. Two cases are presented in each figure; one allows negative pressure and the other does not (imposing Reynolds-Swift-Stieber boundary conditions). The pressure profiles for each case are presented in Figures 16, 17, 18, and 19.

The total friction of the six thrust pads was summed and then divided by total load to obtain the friction coefficient for a series of $\mu U/PB$ values and plotted for comparison with experimental results. Figure 20 shows the resulting friction curve and Figure 21 the minimum film thickness predicted by the computer program as a function of $\mu U/PB$ when negative pressures are allowed and not allowed.

THIS CALCULATION ALLOWED NEGATIVE PRESSURES
SLOPE=1. 745784971E-4 PIVOT=0. 5, 0.32
CENT. PRESS=0.499870509989
PURE HYDRO LOAD=1152.87613215
MIXED HYDRO LOAD=0 PSI
CONTACT LOAD=0 PSI
TOT. LOAD=1152. 87613215 PSI
PURE HYDRO FRICT=0.455753962741 PSI
MIXED HYDRO FRICT=0 PSI
CONTACT FRICT=0 PSI
TOT. FRICT=0.455753962741 PSI
U-ETA/W=2.146978267E-8
COEF. OF FRICTION =5.698976039E-4
SHOE SPEED=9.52952. IN/S
PRESS. MOM. =-0.0663837265664 FT LB/IN
SHEAR MOM. =0.0648519658822 FT-LB/IN
H1/H2 RATIO=3.70320940581
H2=1. 491842724E-4
C/H2=0. 234609181239
ABRAMOVITZ'S PHI=1. 34062389279
MIN. MACRO FILM HEIGHT=1. OE-41N. AT X/B=0.752047705209
NO. ITERATIONS=4
NO MIXED LUBRICATION
PLOT #2

THIS CALCULATION DID NOT ALLOW NEGATIVE PRESSURES
SLOPE=1.564805208E-4 PIVOT =0. 5, 0.32
CENT. PRESS=0.499974779391
PURE HYDRO LOAD=1206.30136639
MIXED HYDRO LOAD=0 PSI
CONTACT LOAD=0 PSI
TOT. LOAD=1206.30136639 PSI
PURE HYDRO FRICT=0. 450305088924 PSI
MIXED HYDRO FRICT=0 PSI
CONTACT FRICT=0 PSI
TOT. FRICT=0.450305088924 PSI
U-ETA/W=2. 051891898E-8
COEF. OF FRICTION =5.297745429E-4
SHOE SPEED=9.52952 IN/S
PRESS. MOM. =-0.0135286387374 FT LB/IN
SHEAR MOM. =0.0640766129335 FT-LB/IN
H1/H2 RATIO=3. 25782683417
H2=1. 600964244E-4
C/H2=0.218618249131
ABRAMOVITZ'S PHI=1. 24924713789
MIN. MACRO FILM HEIGHT=1. OE-4IN. AT X/B=0. 725918751951
NO. ITERATIONS=3
REYNOLDS-SWIFT-STIEBER CAVITATION CONDITION IMPOSED
NO MIXED LUBRICATION
PLOT #3

Figure 14 - Typical Computer Output Under
Hydrodynamic Lubrication Conditions

27

THIS CALCULATION DID NOT ALLOW NEGATIVE PRESSURES
SLOPE=1. 15566044E-4 PIVOT =0. 5, 0.32
CENT. PRESS=0. 499920907264
PURE HYDRO LOAD=3679. 03496371
MIXED HYDRO LOAD=1386. 29530187 PSI
CONTACT LOAD=0.194436872283 PSI
TOT. LOAD=5065. 52470245 PSI
PURE HYDRO FRICT=0. 9356570736 PSI
MIXED HYDRO FRICT=0. 246750572852 PSI
CONTACT FRICT=0. 0388873744566 PSI
TOT. FRICT=1. 22129502091 PSI
U-ETA/W=4. 886364484E-9
COEF. OF FRICTION=3.566654547E-4
SHOE SPEED=9. 52952 IN/S
PRESS. MOM. =-0.178157352734 FT LB/IN
SHEAR MOM. =0.173785396295 FT-LB/IN
H1/H2 RATIO=3. 24726979178
H2=1. 187919504E-4
C/H2=0. 294632758297
ABRAMOVITZ'S PHI=1. 6836157617
MIN. MACRO FILM HEIGHT=3. OE-5IN. AT X/B=0. 666848475978
NO. ITERATIONS=4
REYNOLDS-SWIFT-STIEBER CAVITATION CONDITION IMPOSED
MIXED LUBRICATION WITHIN59AND74.501%
PLOT #10

THIS CALCULATION ALLOWED NEGATIVE PRESSURES
SLOPE=1. 86915756E-4 PIVOT =0.5, 0.32
CENT. PRESS=0. 499818277712
PURE HYDRO LOAD=3127. 8232727
MIXED HYDRO LOAD=1254. 44868354 PSI
CONTACT LOAD=3. 72204560221 PSI
TOT. LOAD=4385. 99400184 PSI
PURE HYDRO FRICT=1. 06370550783 PSI
MIXED HYDRO FRICT=0. 465346373011 PSI
CONTACT FRICT=0.744409120441 PSI
TOT. FRICT=2. 27346100128 PSI
U-ETA/W=5. 64341857-9
COEF. OF FRICTION =7.052614264E-4
SHOE SPEED=9. 52952 IN/S
PRESS. MOM. =0.354420588933 FT LB/IN
SHEAR MOM. =0. 323504406638 FT-LB/IN
H1/H2 RATIO=7. 40885652335
H2=6. 737167461E-5
C/H2=0. 519506160446
ABRAMOVITZ'S PHI=2. 96860663112
MIN. MACRO FILM HEIGHT=2. 5E-5IN. AT X/B=0. 7698596227
NO. ITERATIONS=4
MIXED LUBRICATION WITHIN66AND88. 001%
PLOT #11

Figure 15 - Typical Computer Output Under
Mixed Lubrication Conditions

28
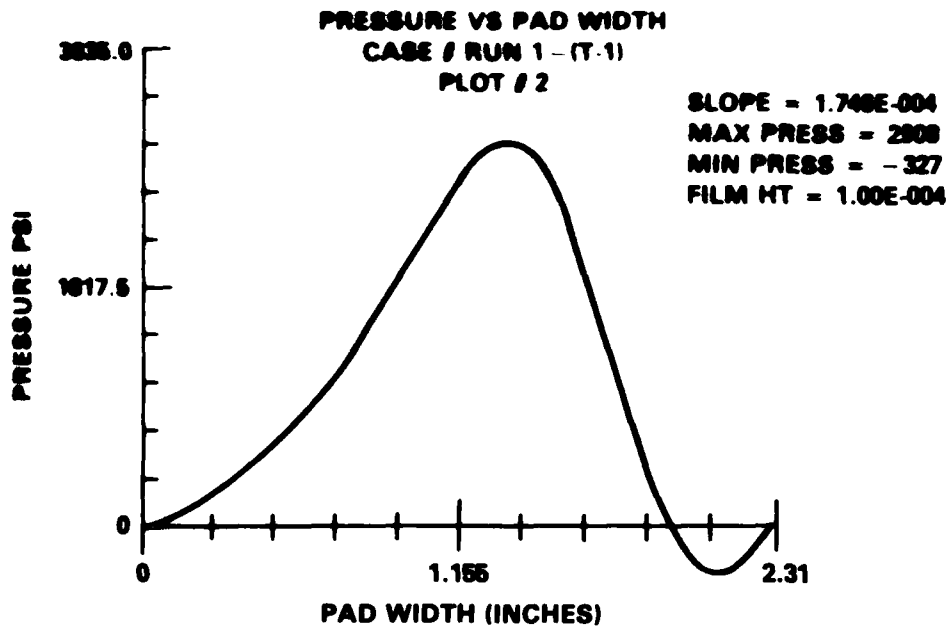
Figure 16 - Pressure Distribution under Hydrodynamic
Lubrication Conditions allowing Negative Pressures
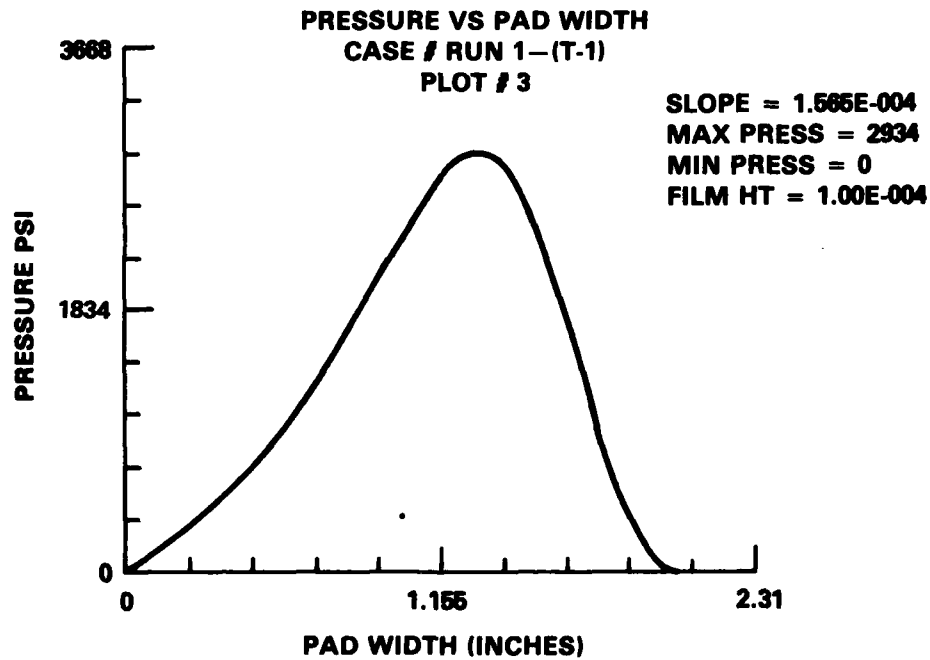
Figure 17 - Pressure Distribution under Hydrodynamic
Lubrication Conditions with Reynolds-Swift-Stieber
Boundary Conditions

29

PRESSURE VS PAD WIDTH
CASE # RUN 1– (T-1)
PLOT # 10

SLOPE = 1.156E-004
MAX PRESS = 18022
MIN PRESS = 0
FILM HT = 3.00E-005
MIXED LUBRICATION
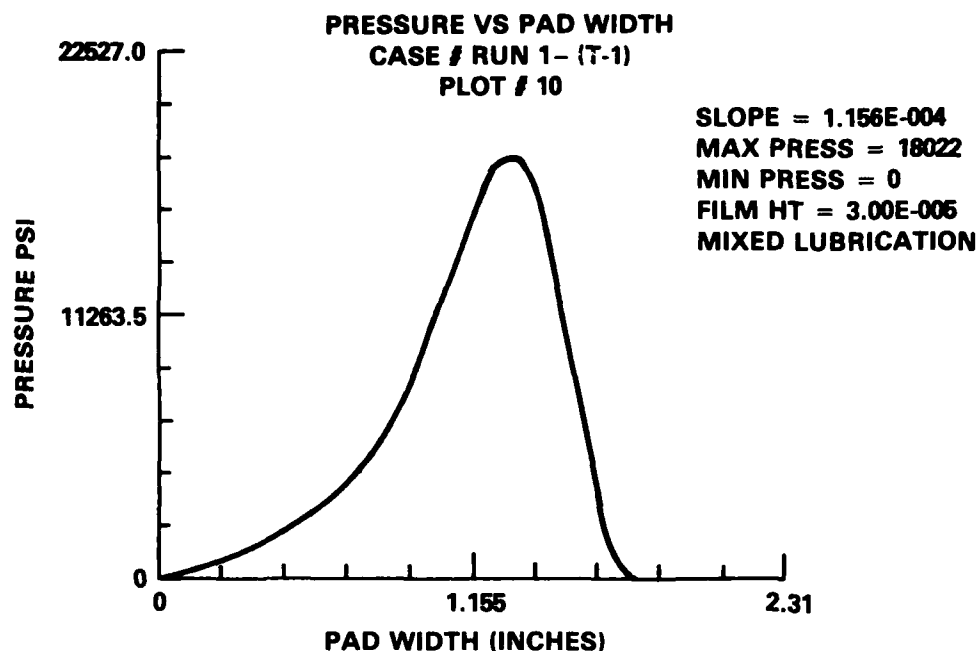
Figure 18 – Pressure Distribution under Mixed
Lubrication Conditions with Reynolds-Swift-
Stieber Boundary Conditions

PRESSURE VS PAD WIDTH
CASE # RUN 1–(T-1)
PLOT # 11

SLOPE = 1.869E-004
MAX PRESS = 21317
MIN PRESS = –9406
FILM HT = 2.50E-005
MIXED LUBRICATION

Figure 19 – Pressure Distribution under Mixed
Lubrication Conditions allowing
Negative Pressures
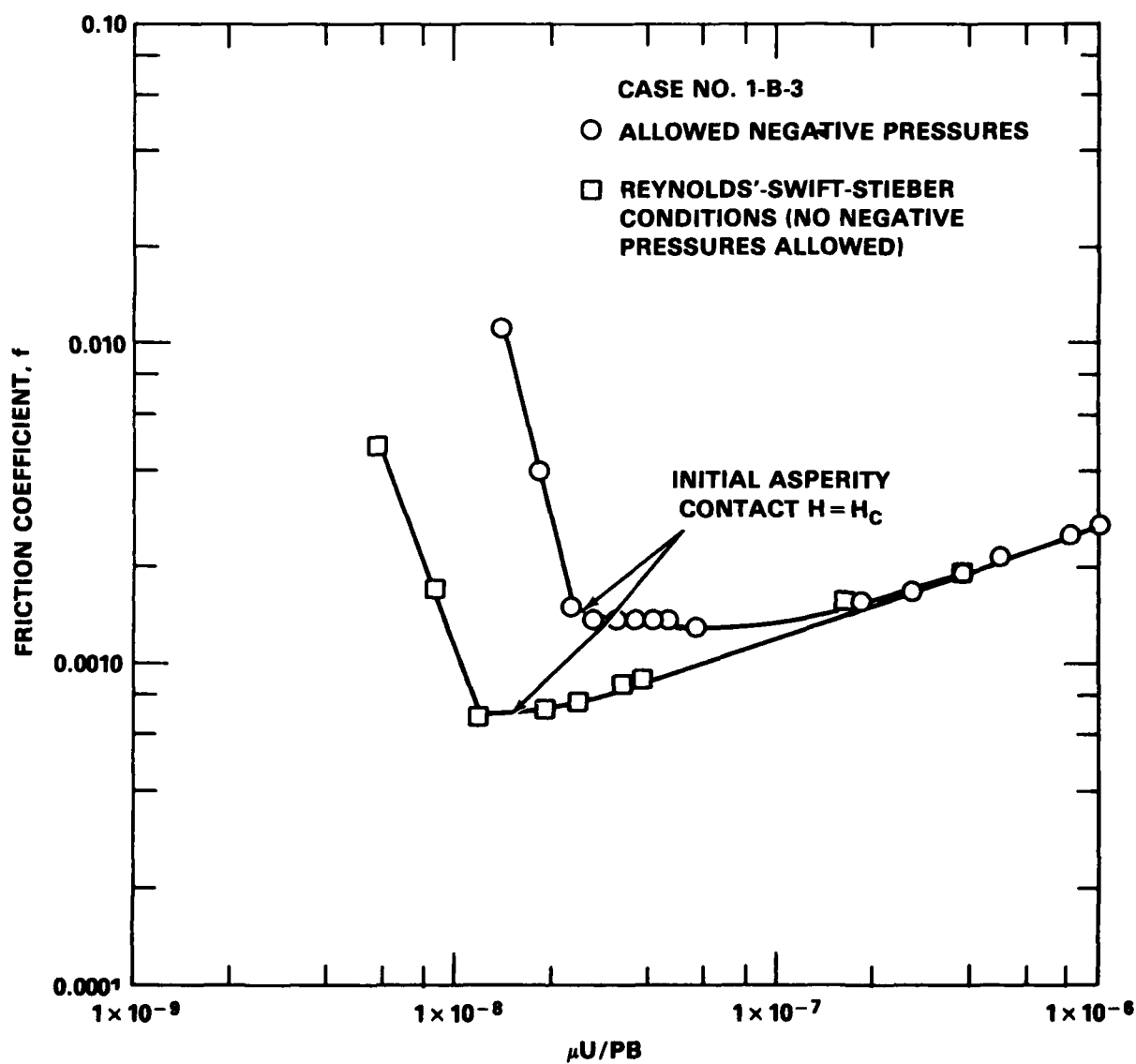
Figure 20 – Theoretical Friction Coefficients Versus Parameter μU/PB allowing
Negative Pressure and Applying Reynolds-Swift-Stieber Boundary Conditions
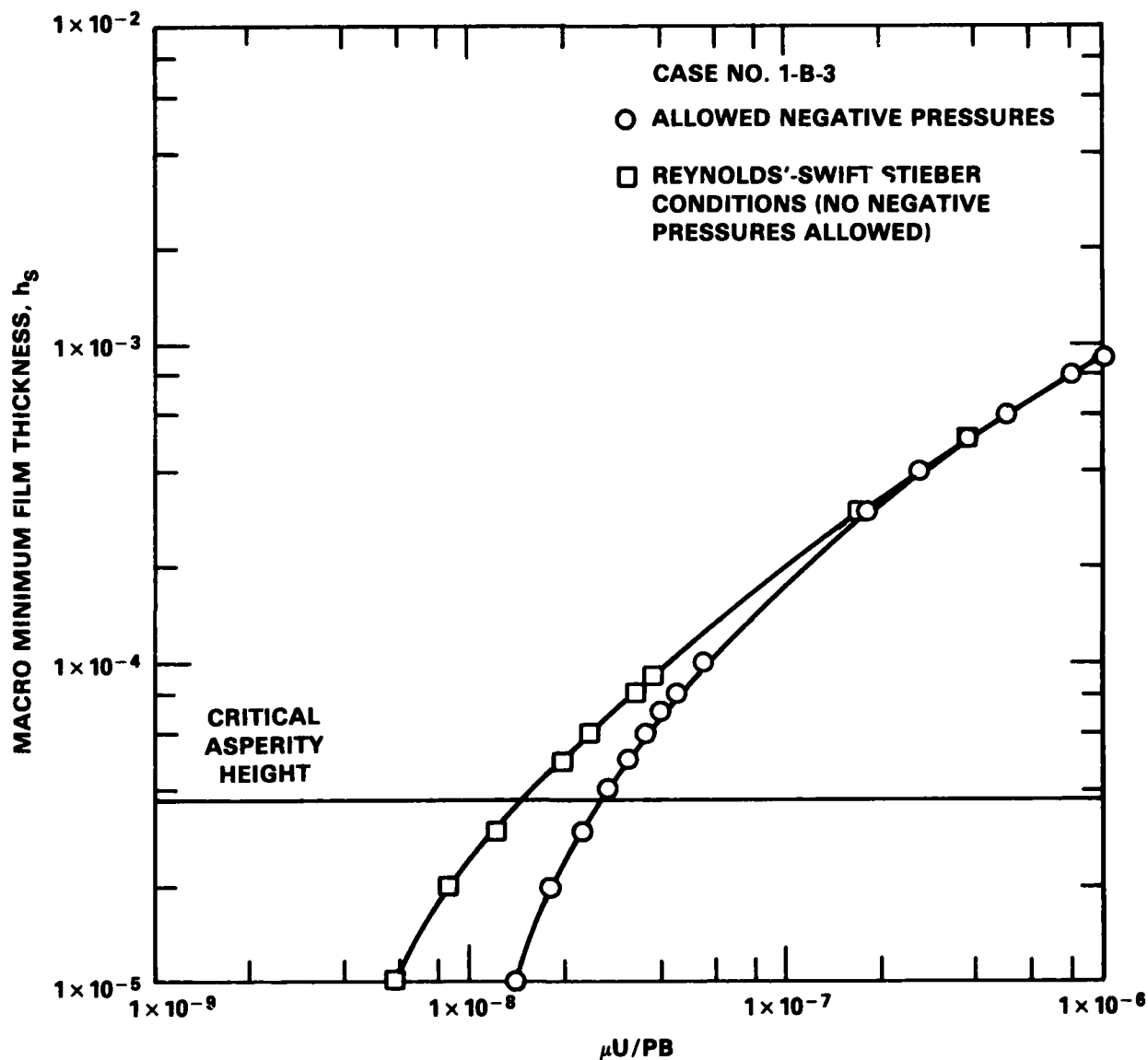
Figure 21 - Theoretical Minimum Film Thickness Versus Parameter μU/PB Allowing
Negative Pressure and Applying Reynolds-Swift-Stieber Boundary Conditions

EXPERIMENTAL RESULTS

After topographical analysis of the bearing and mating surfaces, the bearing test machine was assembled. A standard Navy lubricant for thrust bearings, 2190 TEP, was used in the first test sequence. The viscosity at two reference temperatures (104°F and 212°F) and the specific gravity at 60°F were determined for a sample from the oil used in the experiment. The viscosity at other temperatures was obtained using ASTM standard viscosity-temperature charts[8] for liquid petroleum (see Figure 22). The first runs were made at ambient oil temperatures. (No external heat was added to the lubricant during the test). The speed of the test machine was set to a nominal 35 rpm with no applied bearing l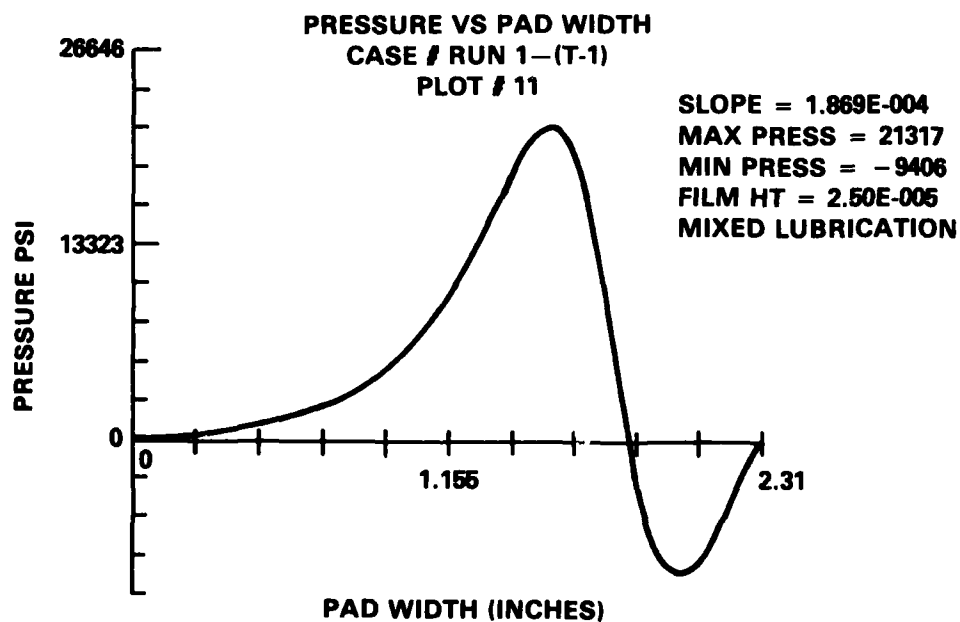oad. Loads were applied in increments of approximately 75 psi bearing unit load up to about 450 psi. Torque and other data were recorded immediately after a change in load and after 15 min operation at each load. Other parameters recorded were time of test, rotational speed, load cell readings, temperature of the bulk oil, temperature of oil near bearing outlet, water sump temperature, and bearing torque. Table 6 shows results of the ambient temperature runs.

The model predicts that there should be hydrodynamic behavior when $\mu U/PB$ exceeds 2×10^{-8}, according to Figures 20 and 21. The lowest $\mu U/PB$ value reached in the ambient test sequence was 2×10^{-7}. The lubricant was heated to 150°F to reduce the viscosity so that lower values of $\mu U/PB$ could be reached while speed and load conditions were maintained within reasonable limits. The lubricant used as in the ambient temperature runs was heated by circulating water through the coils in the oil sump. Table 7 shows results of the higher temperature runs. Although $\mu U/PB$ of 3.5×10^{-8} was reached, the friction data still appeared to be obeying hydrodynamic principles.

TABLE 6 – DATA FROM RUN 1 – 2190 TEP at AMBIENT TEMPERATURE

Test Description	Time On (hr)	Time Off (hr)	Speed N (rpm)	Speed U (in/s)	Load Cell Readings (lb)			Total Load Cells (lb)	Bearing Load (psi)	Bulk Oil Temperature (°F)	Oil Viscosity (cs)	Oil Viscosity (Reyns)	μU/PB	Torque in-lb	$f=\frac{T}{2FR}$ *
3 Pad Thrust Bearing with 2190 TEP Oil at Room Temperature	1310		35	9.63	333	280	320	933	75.85	73	260	32×10^{-6}	1.74×10^{-6}	72.23	14.7×10^{-3}
		1325	36	9.9?	?03	250	290	843	68.54	74	260	32×10^{-6}	2×10^{-6}	63.89	$14.4 \times 10^{-?}$
	1328		36	9.9?	610	520	590	1720	139.84	75	250	31×10^{-6}	9.0×10^{-7}	108.34	12×10^{-3}
		1343	36	9.9?	585	500	560	1645	133.74	76	250	31×10^{-6}	1.0×10^{-6}	97.23	11.3×10^{-3}
	1347		36	9.90	950	820	910	2680	217.9	76	240	30×10^{-6}	5.8×10^{-7}	136.12	9.7×10^{-3}
		1402	36	9.90	930	800	880	2610	₋12.2	77	240	30×10^{-6}	5.99×10^{-7}	125.01	9.1×10^{-3}
	1405		36	9.90	1250	1090	1200	3540	287.8	77	220	27×10^{-6}	3.98×10^{-7}	144.46	7.8×10^{-3}
		1420	36	9.90	1230	1080	1180	3490	283.7	79	220	27×10^{-6}	4.03×10^{-7}	130.57	7.1×10^{-3}
	1423		36	9.90	1570	1380	1520	4470	363.4	79	210	26×10^{-6}	3.03×10^{-7}	161.12	6.8×10^{-3}
		1435	36	9.90	1560	1375	1500	4435	360.6	80	210	26×10^{-6}	3.06×10^{-7}	144.46	6.2×10^{-3}
	1440		36	9.90	2040	1810	1990	5840	474.8	81	200	24×10^{-6}	2.14×10^{-7}	183.35	6.0×10^{-3}
		1450	36	9.90	2040	1800	1980	5820	473.2	82	200	24×10^{-6}	2.15×10^{-7}	161.12	5.3×10^{-3}

TABLE 7 – DATA FROM RUN 2 – 2190 TEP AT 150°F

| Test Description	Time On (hr)	Time Off (hr)	Speed N (rpm)	Speed U (in/s)	Load Cell Readings (lb)			Total Load Cells (lb)	Bearing Load (psi)	Bulk Oil Temperature (°F)	Oil Viscosity (cs)	Oil Viscosity (Reyns)	μU/PB	Torque in-lb	$f=\frac{T}{2FR}$ *
3 Pad Thrust Bearing with 2190 TEP Oil at 150°F	1257		36.5	10.04	340	300	292	932	75.77	148	27	3.3×10^{-6}	1.87×10^{-7}	16.67	3.41×10^{-3}
		1312	36.5	10.04	308	267	255	830	67.48	153	25	3.1×10^{-6}	1.97×10^{-7}	12.22	2.81×10^{-3}
	1316		36	9.90	610	550	545	1705	138.62	154	24	2.9×10^{-6}	8.87×10^{-8}	27.78	3.10×10^{-3}
		1331	36	9.90	590	520	520	1630	132.52	155	24	2.9×10^{-6}	9.27×10^{-8}	22.22	2.6×10^{-3}
	1335		36	9.90	935	840	845	2620	213	154	24	2.9×10^{-6}	5.77×10^{-8}	38.89	2.83×10^{-3}
		1350	36	9.90	890	800	800	2490	202.4	145	30	3.6×10^{-6}	7.54×10^{-8}	36.11	2.76×10^{-3}
	1354		36	9.90	1240	1125	1150	3515	285.8	144	30	3.6×10^{-6}	5.34×10^{-8}	50	2.71×10^{-3}
		1409	36	9.90	1190	1080	1110	3380	274.8	143	30	3.6×10^{-6}	5.55×10^{-8}	44.45	2.50×10^{-3}
	1412		36	9.90	1545	1400	1445	4390	357	143	30	3.6×10^{-6}	4.27×10^{-8}	58.34	2.53×10^{-3}
		1427	36	9.90	1525	1380	1440	4345	353.3	146	30	3.6×10^{-6}	4.32×10^{-8}	50	2.19×10^{-3}
	1429		36	9.90	1875	1690	1785	5350	435	147	28	3.5×10^{-6}	3.41×10^{-8}	63.89	2.27×10^{-3}
		1444	36	9.90	1870	1710	1775	5355	435.4	150	26	3.2×10^{-6}	3.11×10^{-8}	50	1.78×10^{-3}
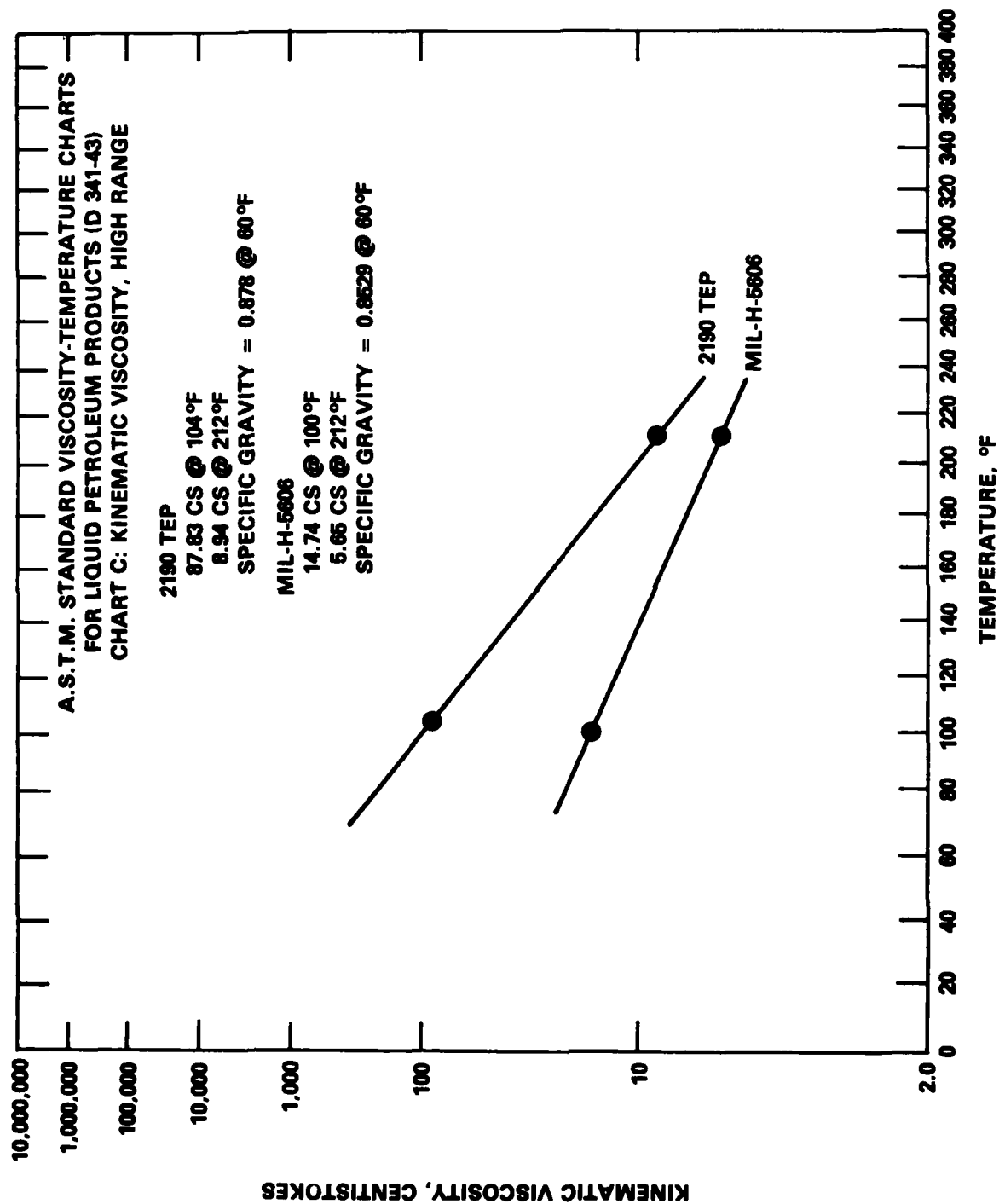
Figure 22 – Viscosity-Temperature Relationship for MS 2190 TEP Oil and
MIL-H-5606 Hydraulic Fluid

35

A low viscosity fluid was sought to extend the test to lower values of $\mu U/PB$. A hydraulic fluid meeting MIL-H-5606[9] was selected. The viscosity-temperature relationship for a sample of the MIL-H-5606 fluid was obtained and plotted in Figure 22. These fluids exhibit non-Newtonian behavior and break down under high shear rates.[10] While the fluid is non-Newtonian at about 59°F, its behavior at 100°F approaches Newtonian. The shear rate at $\mu U/PB$ of 2×10^{-8} for the computerized model with Reynolds'-Swift-Stieber cavitation condition produces a shear rate of 16×10^4 reciprocal seconds. The viscosity loss due to shear should amount to only 10%. The fluid was heated to about 100°F and tests conducted in the bearing machine in a similar manner to those described earlier. The results of those tests are listed in Table 8.

The data from the three test runs are compared to the computer-generated results in Figure 25. The friction coefficient is defined by the following expression:

$$T = fFR$$

where: T is the torque in in-lb,

f is the friction coefficient,

F is the total applied thrust load,

and R is the radius to the pad center.

The measured torque on the test machine is divided by two because it is the result of two sets of bearings. The data for the 2190 TEP oil in both ambient and 150°F runs are parallel to the predicted values and apparently operating hydrodynamically, but the magnitude of the friction measured is about four times the value predicted. The results with the MIL-H-5606 fluid indicate that the bearings were operating in mixed lubrication conditions.

TABLE 8 - DATA FROM RUN 3 - MIL-H-5606 FLUID AT 105°F

| Test Description	Time On (hr)	Time Off (hr)	Speed N (rpm)	Speed U (in/s)	Load Cell Readings (1b)	Total Load Cells (1b)	Bearing Load (psi)	Bulk Oil Temperature (°F)	Oil Viscosity (cs)	Oil Viscosity (Reyns)	$\mu U/PB$	Torque in-lb	$f=\dfrac{T}{2FR}$ *
3 Pad Thrust	914		32	8.8	370 335 325	1030	83.75	104	14	1.7×10^{-6}	7.64×10^{-8}	37.78	7×10^{-3}
Bearing		929	30	8.25	320 285 270	875	71.14	105	14	1.7×10^{-6}	8.44×10^{-8}	15	3.3×10^{-3}
with MIL-													
H-5606	934		29	7.98	625 570 560	1755	142.7	106	14	1.7×10^{-6}	4.07×10^{-8}	96.12	10.4×10^{-3}
Fluid		949	29.5	8.11	585 530 525	1640	133.3	107	13	1.6×10^{-6}	4.17×10^{-8}	62.78	$7.3 \times 10_{-3}$
	933		29.5	8.11	930 850 870	2650	215.5	107	13	1.6×10^{-6}	2.10×10^{-8}	165.6	11.9×10^{-3}
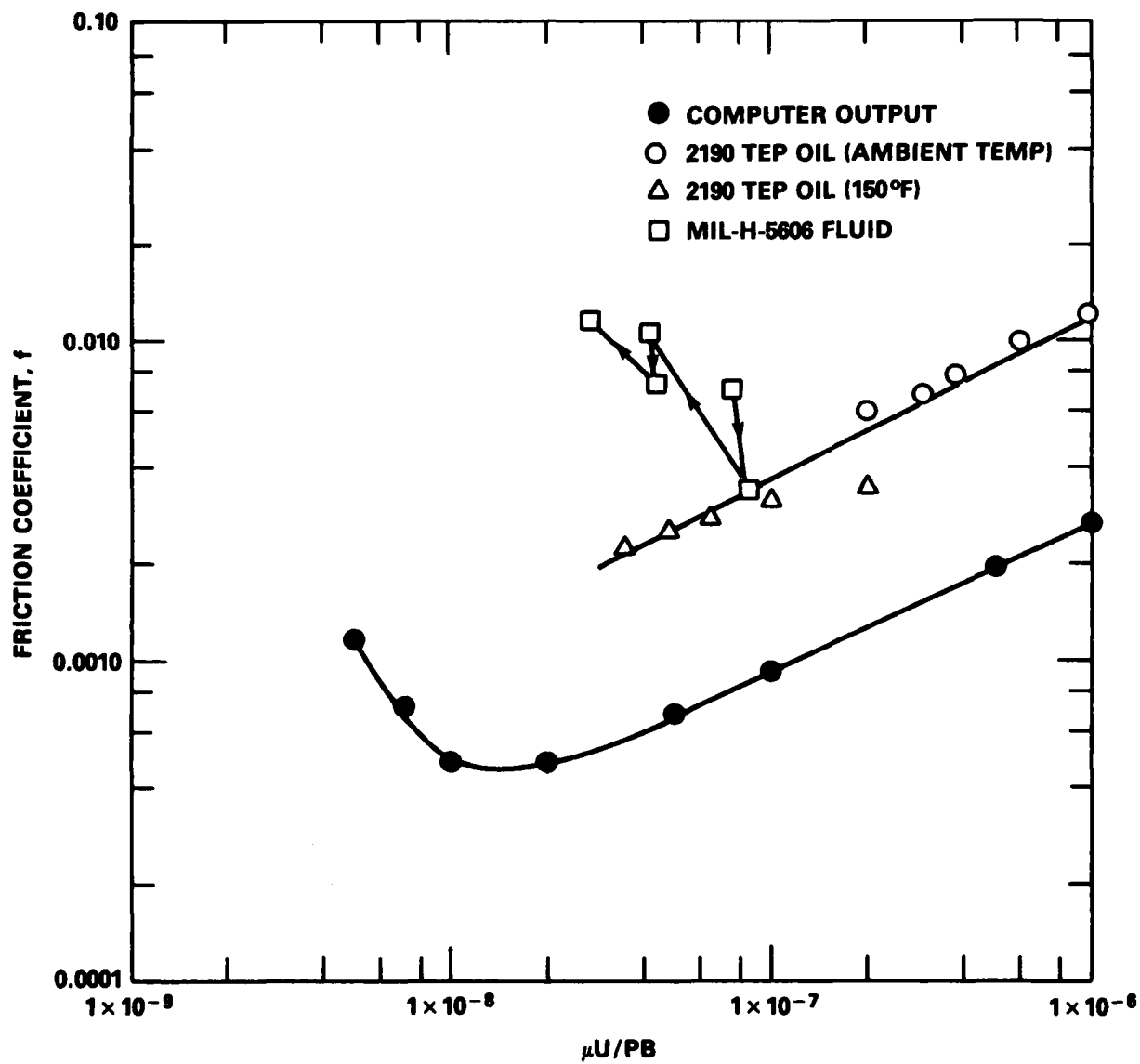
Figure 23 – Comparison of Measured and Computed Friction Coefficient for Crowned Tilt-Pad Thrust Bearing Having Longitudinal Roughness (Precise Measured Values are Shown in Tables 6-8)

DISCUSSION

The friction coefficients measured under hydrodynamic conditions during the experiment using the 2190 TEP turbine oil were about four times those predicted by the computer model under hydrodynamic conditions. Both the ambient and 150°F temperature runs using that oil exhibited friction representative of a complete hydrodynamic lubricant film separating the surfaces.

We suspect that of the assumptions made in the theoretical model, that for neglecting of side leakage would have influenced the results most significantly. Fuller[11] pointed out the significant influence of side leakage. He presented side leakage correction factors for the load and film thickness expressions describing a simple fixed inclined flat bearing that has an inlet film thickness of double the outlet film thickness. He modified his derived expressions for bearing load and minimum film thickness by a side leakage factor, η, as follows:

$$W = \frac{6\mu U l^2 B \eta K_p}{h_o^2}$$

$$\text{and } h_o = \sqrt{\frac{6\mu U l \eta K_p}{P_{avg}}}$$

The side leakage factors were based upon experiments of Kingsbury and Needs (as cited by Fuller[11]) and are a function of the bearing length to width ratio. The coefficient of friction for Fuller's bearing configuration is given by:

$$f = \frac{F_R}{W} = \frac{\mu B l U K_{f_r}}{h_o}$$

It is proportional to $\eta^{-1/2}$. According to Fuller, the correction factor, η, for side leakage for the thrust bearings evaluated in our work is 0.32. Thus the calculated friction should be multiplied by $(0.32)^{-1/2}$ or 1.77 to yield a better value for comparison with measured friction.

Correcting for side leakage would account for nearly half of the difference between our predicted and measured results. In addition, the thrust pads used in our study were crowned both in the direction of motion and in the radial direction. Under these conditions, it is conceivable that side leakage correction could account for the four-fold difference between the friction coefficients.

38

The model assumed a parabolic surface for each bearing. The topographical measurements, however, showed that not all bearing surfaces could be represented by a simple parabola. The capacity to input varying shapes of the bearing surface is needed. Accordingly we have begun work with Dr. C. Pan of Columbia University (N00167-82-C-0134) which includes studies of side leakage and variable pad shapes. Dr. Pan's model is a thrust pad with a 20 x 20 finite element grid. Surface shapes can be set by the initial values given to the 400 grid points.

Thermo-elastic effects should be considered in the development of a more sophisticated model because thermal and elastic distortions change the shapes of the thrust pad surfaces. Some work has been done in these areas. A finite element model has been developed to determine the distortions due to thermal gradients within the thrust pad.[12] Under normal (hydrodynamic) conditions, lubricant shear and minor asperity contact generate heat. Some of the heat is absorbed by the fluid or through the load zone; the rest is carried away through the thrust pad. The surface temperature at the film would be hottest and there is a thermal gradient through the thickness of the pad. This gradient would increase the initial crown and the crown caused by pressure loading on the face. Thus, heat transfer must be analyzed to develop the temperature profile in the thrust pad. A preliminary finite element study of heat transfer under hydrodynamic lubrication[13] has been conducted under this program. A general analysis of interactive mechanisms of sliding-surface bearings was presented by Daugherty and Pan.[5] However, additional work is needed in elasto-hydrodynamics, before the results can be incorporated into our model.

The tests conducted with the MIL-H-5606 fluid resulted in frictional behavior typical of the mixed-lubrication regime. The non-Newtonian effects were much greater than expected. In Figure 23, the friction coefficients were plotted against a $\mu U/PB$ value based upon measurements of the kinematic viscosity of the fluid. The kinematic viscosity is determined by measuring the time for the liquid to flow under gravity through a glass viscometer and thus does not consider high shear rates such as those of the experiment. The viscosity of the MIL-H-5606 fluid would need to be about one third of the value used for the friction data shown in Figure 23 to fit the curve expected.

Asperity interactions occurred during the runs with MIL-H-5606 fluid. Wear was apparent during the 15 min operation at a given load. The resulting decrease in friction coefficient may have been caused by the polishing of high asperities.

39

The arrows in Figure 23 show the sequence of tests conducted for the MIL-H-5606 fluid. The friction coefficient decreased after 15 min under given load, then increased when additional load was applied. Furthermore, the model as presently structured does not consider the contribution of the mechanical-chemical inter-actions of the surfaces with the fluid and its additives that occur in the mixed and boundary lubrication zones.

Studies are being conducted at Mississippi State Universit_ by Dr. A. Stiffler (DTNSRDC Contract N61533-83-M-2799) to predict the load support and friction coef-ficient in sliding pairs when an ensemble of asperities is operating in near contact. Dr. Stiffler's analysis will include one dimensional microtopographic studies for an asperity against a flat surface and an asperity against another asperity, for elastic deformations of asperities, for non-Newtonian lubricants, and for temperature effects.

CONCLUSIONS

Measured friction of a crowned tilt-pad thrust bearing with longitudinal roughness when plotted against the $\mu U/PB$ parameter was parallel to but higher than the results predicted by the model under hydrodynamic lubrication conditions.

We now believe that major differences were due primarily to the neglect of side leakage in the model. Additional improvements could be made to the model by consid-ering variable viscosity in the film and different film shapes. The present model cannot handle the complex tribological interactions that occur in experiments in the mixed and probably in the boundary lubrication regimes of tilt-pad thrust bearings.

RECOMMENDATIONS

The present model should be expanded to consider side leakage effects, variable viscosity, thermo-elastic deformations, pad shapes, skewed roughness patterns, and improved local asperity configurations for a tilt-pad bearing operating under hydro-dynamic and mixed lubrication. Also, more detailed studies are needed of the local behavior of asperities under concentrated loads. Finally, additional experiments are needed to verify some of the assumptions in the present model. Such experiments will isolate the effects of selected parameters on the tribological system and lead to a better understanding of the mechanisms involved, be they physical, chemical or (as expected) a combination of both.

ACKNOWLEDGEMENTS

REFERENCES

1. Czichos, H., "Tribology—a systems approach to the science and technology of friction, lubrication, and wear," Elsevier Scientific Publishing Company, Second ed., New York, p. 131 (1979).

2. O'Connor, J. and J. Boyd, "Standard Handbook of Lubrication Engineering," McGraw-Hill Book Company, New York (1968).

3. Raimondi, A. A., "The Influence of Surface Profile on the Load Capacity of Thrust Bearings with Centrally Pivoted Pads," Am. Soc. Mech. Eng. Trans Vol. 77, p. 321 (1955).

4. Christensen, H., "A Theory of Mixed Lubrication," Institution Mech Eng., Vol. 186, No. 41 (1972).

5. Daugherty, T. and C. Pan, "Interactive Mechanisms of Sliding-Surface Bearings," DTNSRDC Report 82/119 (Aug 1983).

6. Pan, C., "Dynamic Analysis of Rupture in These Fluid Films, I-A Nominated Theory," Am. Soc. Mech. Eng. paper ASME 81-Lub-24 (1981).

7. Etsion, I. and L. Ludwig, "Observation of Pressure Variation in the Cavitation Region of Submerged Journal Bearings," Nat. Aeron. Space Admin. NASA Tech Memo 81582 (Oct 1981).

8. American Society for Testing and Materials, "Viscosity-Temperature Charts for Liquid Petroleum Products," ASTM Standard D341 (1982).

9. Military Specification "Hydraulic Fluid, Petroleum Base; Aircraft, Missile, and Ordnance," MIL-H-5f (30 Sep 1971).

10. American Society for Testing and Materials, Symposium on Hydraulic Fluids, ASTM Special Technical Publication No. 267, pp. 95-97.

11. Fuller, D. "Theory and Practice of Lubrication for Engineers," John Wiley & Sons New York (1956).

12. Ma, J., "The Development of a Thermal Distortion Code Using the Finite Element Model," DTNSRDC Report 82/050 (Jun 1982).

13. Bai, K., "Finite-Element Method for Heat Transfer Problem in Hydrodynamic Lubrication," DTNSRDC Report SPD 1043-01 (Apr 1982).

INITIAL DISTRIBUTION

NAVSEA
3 SEA 56X4 (Petros, Graham,
          Fischer)

12 DTIC

CENTER DISTRIBUTION

Copies	Code	Name
3	012	D. Moran
1	1542	
1	1730	J. Ma
1	1844	S. Dhir
1	27	R. Allen
1	272	T. Doyle
1	2723	B. Neild
1	28	Belt
2	283	H. Singerman
1	2832	J. Dray
10	2832	T. Daugherty
10	5211.1	Reports Dist.
1	522.1	TIC (C)
1	522.2	TIC (A)

DTNSRDC ISSUES THREE TYPES OF REPORTS

1. DTNSRDC REPORTS, A FORMAL SERIES, CONTAIN INFORMATION OF PERMANENT TECH-
NICAL VALUE. THEY CARRY A CONSECUTIVE NUMERICAL IDENTIFICATION REGARDLESS OF
THEIR CLASSIFICATION OR THE ORIGINATING DEPARTMENT.

2. DEPARTMENTAL REPORTS, A SEMIFORMAL SERIES, CONTAIN INFORMATION OF A PRELIM-
INARY, TEMPORARY, OR PROPRIETARY NATURE OR OF LIMITED INTEREST OR SIGNIFICANCE.
THEY CARRY A DEPARTMENTAL ALPHANUMERICAL IDENTIFICATION.

3. TECHNICAL MEMORANDA, AN INFORMAL SERIES, CONTAIN TECHNICAL DOCUMENTATION
OF LIMITED USE AND INTEREST. THEY ARE PRIMARILY WORKING PAPERS INTENDED FOR IN-
TERNAL USE. THEY CARRY AN IDENTIFYING NUMBER WHICH INDICATES THEIR TYPE AND THE
NUMERICAL CODE OF THE ORIGINATING DEPARTMENT. ANY DISTRIBUTION OUTSIDE DTNSRDC
MUST BE APPROVED BY THE HEAD OF THE ORIGINATING DEPARTMENT ON A CASE-BY-CASE
BASIS.